Final Technical Report

ON

Designing of Fly Ash Composites in Building Materials for Energy Conservation & Shielding Applications

Dr. Sangeeta Tiwari
Associate Professor and Head
Department of Applied Chemistry
AIAS, Amity University
Noida-201303

Dr. S.K. Dhawan
Scientist G
CSIR-National Physical Laboratory
New Delhi-110012

Ministry of Environment, Forest and Climate Change
Government of India

Dr. M. Raina
Director (C&T)
Ministry of Environment, Forest and Climate Change

ACKNOWLEDEMENT

We are grateful to Clean Technology Division of the Ministry of Environment, Forests & Climate Change, Government of India for sanctioning this project on, "**Modification and Designing of Fly-ash composites in building materials for energy conservation and shielding applications".**

We are highly grateful to Mr. Ashok Lavasa, Secretary, MOEF&CC, Mr. M. M. Kutty, IAS, Additional Secretary, MOEF&CC, Dr. Rashid Hasan, Adviser, MOEF & CC and Dr. M. Raina, Director, MOEF & CC whose ideas, initiatives and decisions became a building force to us. We are also grateful to Dr. M. Salauddhin, Director, MoEF in whose initiative, this project was undertaken. We are indeed grateful to Dr. H. Kharkwal, Scientist, MoEF and Piyali Bandyopadhyay, Project Scientist, MoEF who helped us in final execution of the project.

We extend our special thanks to Prof. Chander Sekhar, Director, National Physical Laboratory, New Delhi, Dr. A.M. Biradar, HOD, Materials Physics & Engineering Division, NPL, Dr. Rajeev Chopra, Head, HRD Group, NPL, Dr. T.D. Senguttuvan, Head, Project Monitoring and Planning, NPL and Sh. M.K. Goyal, COFA, Accounts & Audit Officer, NPL whose timely support and proper advise has helped in timely achieving our goals. We would also like to thank Dr. Ashok K. Chauhan, Founder President, Amity University Uttar Pradesh, whose passion for research and innovation is the driving force for every research activity at Amity. His motivation and words of appreciation helped us in putting our best efforts in the successful conduct of this project. Our sincere gratitude to Prof. (Dr.) Balvinder Shukla, Vice Chancellor, Amity University, whose constant encouragement and guidance helped us in the smooth sailing of the project. Thanks are also due to Prof. **(**Dr.) A.L. Verma, Advisor, Science and Technology Research, Amity University and Prof. (Dr.) Sunita Rattan, Additional Director, Amity Institute of Applied Sciences, Amity University whose timely advice and unconditional support helped in smooth running of the project.

We would also like to acknowledge the support and guidance of Prof. Veena Choudahary, Head, Centre for Polymer Science & Engineering, Indian Institute of Technology, Delhi, Dr. D. Kumar, Professor and Head and Chairman of the Project Monitoring Committee, Dr. M.K. Kamat, CEO, M/s Krishna Conchem, Navi Mumbai, Dr. Fehmeeda Khatoon, Depoartment of Chemistry, Jamia Millia Islamia and Dr. Sanjeev Palliwal from Central Pollution Control Board whose constant monitoring of the project and valuable suggestions helped us in smooth functioning of the Project.

CONTENTS

Executive Summary of the Project

Fly-ash is a waste from coal based thermal power stations and is a major environment concern. Its voluminous production in India, presents serious challenge for its disposal and utilization. Concerted efforts by Department/ Agencies of Govt. of India, in this regard, have resulted in development of new technologies for bulk utilization of the waste. Although over the years the utilization of flyash has considerably increased, the production of flyash has also increased with increase in number of thermal power stations and therefore making its disposal a big challenge for the scientist and researchers.

Hence the main emphasis of the project was to design fly-ash composites by surface modification of treated fly ash by forming its core shell composites with inorganic oxides for their use in Near Infrared Reflective coatings for building applications. Moreover details are provided for the characterization of coatings for various properties including reflectivity, specific application properties and other important paint and film characteristics. Preparation of fly ash - titania core-shell composite particles using different techniques was carried out. Whiteness Index of the pigments was measured using Novo- Shade DUO, 45^0/0 Opacity/ Shade Meter. It was observed that thickness of panel increases with increase in the pigment concentration in the epoxy resin which was measured using Positest DFT, Model: DFT-C. Also whiteness index increase with the increase in the pigment percentage and thickness except in the case of untreated flyashand treated fly ash because darkness increases with increase in percentage of pigment concentration in epoxy resin. Diffuse Reflectance Spectra of Chemically modified fly ash (CMFA) shows a good reflectivity of almost 80% in coated sample.

Solar reflective index (SRI) of the samples were determined using ASTM E1980-01 method by calculating the solar reflectance (R*), thermal emittance and wind coefficient to ascertain efficacy of a cool pigment. Materials having highest SRI values are preferred for cool coating applications. Solar Reflective Index of Powder samples indicated that the TiO_2 coated flyash prepared by aqueous method I exhibits highest SRI value of 92 as

compared other materials indicating it to be good NIR reflective materials. The surface modification of flyash is done by coating it with metal oxide i.e. TiO_2 through a simple and economic process and then coatings were prepared by coating this material on the mild steel panels by spray coating technique. The main outcome of the project is the designing of technique for surface modification of Fly ash by forming its core shell with NIR reflective material wherein, core is of Fly ash and shell is of nano titanium dioxide. This work has led to development of energy efficient coatings based on industrial waste with an added advantage of being antiabrasive and anticorrosive in nature.

Moreover, another application of these multiphase composites have been reported which were synthesized by in-situ co-precipitation with conductive filler multi-walled carbon nanotubes (MWCNT) and magnetic filler (ferrofluid). Moreover, emphasis has also been made to design flexible foam possessing both magnetic properties, electrical properties. Fly-ash is incorporated in foam matrix which increases the tensile strength which can be used for electrostatic charge dissipation and can also be used as magnetic foam. One of the objectives of the present project is to develop foam encapsulated with ferrofluid and conducting particles so that the designed flexible polyurethane foam does not lose its mechanical strength and shows magnetic & electrical attributes. The novelty of the work lies in to the preparation of flexible foam by incorporating fly ash in the matrix which is embedded with ferrofluid and conducting materials which can be used for dissipating electrostatic charge and can also be used as magnetic foam. The aim of the work is to design flexible foam possessing both magnetic properties, electrical properties and also fly-ash is incorporated in foam matrix which increases the tensile strength as well as its flame retardancy. PU foam which shows a static decay time of 120-134 sec shows a decrease in static decay time upto 1.87 sec when 40 phr of flyash is added and hardness factor was found to increase from 32 to 66 in Asker F scale which property can be utilized in practical application in designing of PU foam.

Utilization of bulk fly ash is the ultimate goal that has to be achieved by using it in various applications. Scanning electron microscopy results confirm the presence of fly

ash particles covered with ferrofluid nanoparticles along with MWCNTs. Accordingly, the present report also provides a process of designing fly ash tiles by incorporating specific filler materials and expanded graphite which can be used for EMI shielding and antistatic behavior depending upon the loading of conducting matrix which ranges from 1 % to 15 %. The static decay time data shows that 1 % loading of expanded graphite in fly-ash tile completely dissipates the charge from the surface. Similarly on loading 5% percentage of EG in fly-ash completely dissipates the static charge. This shows that 1 % loading of EG in fly-ash tile is good enough for using the tile for antistatic purposes. EMI shielding behavior of the fly-ash tiles incorporated with different loading levels of EG was also carried out in X-band range in order to see how much shielding attenuation of these tiles can be attained when different loadings of EG is incorporated in the fly-ash tile. A shielding effectiveness of 40-45 dB is obtained on loading 20 % of EG which shows that these tiles made with flyash can be used for practical applications where interference from electromagnetic radiation is a big concern to the industries.

Multiphase composites show total shielding effectiveness of 48 dB (>99.998 % attenuation) in the Ku-band (12.4–18 GHz) frequency range. The electromagnetic attributes, dielectric and permeability parameters have been calculated from the measured scattering parameters (S_{11}, S_{22}, S_{12}, S_{21}) using the Nicolson–Ross–Weir algorithm. The synthesized multiphase composites were characterized using XRD, FTIR, VSM and SEM. Our investigation provides distinctive way of utilization fly ash for designing and preparing high-performance EMI shielding materials. PU foam incorporated with flyash not only increases its mechanical strength but also imparts better hardness factor and better flammability and shoes a static decay time of 1.87 sec which is a positive response towards its utilization for antistatic encapsulating material. Moreover, flyash based tiles can be effectively used for antistatic and EMI shielding applications.

INTRODUCTION

This report describes the designing of fly-ash composites by surface modification of treated fly ash by forming its core shell composites with inorganic oxides for their use in Near Infrared Reflective coatings for building applications. Moreover details are provided for the characterization of coatings for various properties including reflectivity, specific application properties and other important paint and film characteristics. Moreover, another application of these multiphase composites have been reported which were synthesized by in-situ co-precipitation with conductive filler (MWCNT) and magnetic filler (ferrofluid). Moreover, emphasis has also been made to design flexible foam possessing both magnetic properties, electrical properties. Fly-ash is incorporated in foam matrix which increases the tensile strength which can be used for electrostatic charge dissipation and can also be used as magnetic foam. Utilization of bulk fly ash is the ultimate goal that has to be achieved by using it in various applications. Scanning electron microscopy results confirm the presence of fly ash particles covered with ferrofluid nanoparticles along with MWCNTs. Our investigation provides distinctive way of utilization fly ash for designing and preparing high-performance EMI shielding materials. Multiphase composites show total shielding effectiveness of 48 dB (>99.998 % attenuation) in the Ku-band (12.4–18 GHz) frequency range. The electromagnetic attributes, dielectric and permeability parameters have been calculated from the measured scattering parameters (S_{11}, S_{22}, S_{12}, S_{21}) using the Nicolson–Ross–Weir algorithm. The synthesized multiphase composites were characterized using XRD, FTIR, VSM and SEM.

Fly-ash is a waste from coal based thermal power stations and is a major environment concern. Its voluminous production in India, presents serious challenge for its disposal and utilization. Concerted efforts by Department/ Agencies of Govt. of India, in this regard, have resulted in development of new technologies for bulk utilization of the waste. Although over the years the utilization of flyash has considerably increased, the production of flyash has also increased with increase in number of thermal power

stations and therefore making its disposal a big challenge for the scientist and researchers.

Figure 1. Shows thermal power plants producing fly-ash as a waste material

Fly ash is one of the residues generated in the combustion of coal (Fig. 1). It is an industrial by-product recovered from the flue gas of coal burning electric power plants. Depending upon the source and makeup of the coal being burned, the components of the fly ash produced vary considerably, but all fly ash includes substantial amounts of silica (silicon dioxide, SiO_2) (both amorphous and crystalline) and lime (calcium oxide, CaO). In general, fly ash consists of SiO_2, Al_2O_3, Fe_2O_3 as major constituents and oxides of Mg, Ca, Na, K etc. as minor constituent. Fly ash particles are mostly spherical in shape and range from less than 1 µm to 100 µm with a specific surface area, typically between 250 and 600 m^2/kg. The specific gravity of fly ash vary in the range of 0.6-2.8 gm/cc. Physical properties of fly ash mainly depend on the type of coal burned and the burning conditions. Class F fly ash is generally produced from burning high rank (containing high carbon content) coals such as anthracite and bituminous coals, whereas, Class C fly ash is produced from low rank coals. Fly ash particles are classified into two types, precipitator and cenosphere. Generally, the solid spherical particles of fly ash are called

precipitator fly ash and the hollow particles of fly ash with density less than 1.0 g cm^{-3} are called cenosphere fly ash. One common type of fly ash is generally composed of the crystalline compounds such as quartz, mullite and hematite, glassy compound such as silica glass, and other oxides. The precipitator fly ash, which has a density in the range 2.0–2.5 g cm^{-3} can improve various properties of selected matrix materials, including stiffness, strength, and wear resistance and reduce the density. Cenosphere fly ash, which consists of hollow fly ash particles, can be used for the synthesis of ultra-light composite materials due to its significantly low density, which is in the range 0.4–0.7 g cm^{-3}, compared with the densities of metal matrices, which is in the range of 1.6–11.0 g cm^{-3}. Coal fly ash has many uses including as a cement additive, in masonry blocks, as a concrete admixture, as a material in lightweight alloys, as a concrete aggregate, in flowable fill materials, in roadway/runway construction, in structural fill materials, as roofing granules, and in grouting. The largest application of fly ash is in the cement and concrete industry, though, creative new uses for fly ash are being actively sought like use of fly ash for the fabrication of MMCs.

Chemical composition

Component	Bituminous	Sub bituminous	Lignite
SiO_2	20-60	40-60	15-45
Al_2O_3	5-35	20-30	10-25
Fe_2O_3	10-40	4-10	4-15
CaO	1-12	5-30	15-40
MgO	0-5	1-6	3-10
SO_3	0-4	0-2	0-10

Na_2O	0-4	0-2	0-6
K_2O	0-3	0-4	0-4
LOI	0-15	0-3	0-5

Fly ash material solidifies while suspended in the exhaust gases and is collected by electrostatic precipitators or filter bags. Since the particles solidify while suspended in the exhaust gases, fly ash particles are generally spherical in shape and range in size from 1 μm to 100 μm. They consist mostly of silicon dioxide (SiO_2), which is present in two forms: amorphous, which is rounded and smooth, and crystalline, which is sharp, pointed and hazardous; aluminium oxide (Al_2O_3) and iron oxide (Fe_2O_3). Fly ashes are generally highly heterogeneous, consisting of a mixture of glassy particles with various identifiable crystalline phases such as quartz, mullite, and various iron oxides.

Classification of fly ash

Two classes of fly ash are defined by ASTM C618: Class F fly ash and Class C fly ash. The chief difference between these classes is the amount of calcium, silica, alumina, and iron content in the ash. The chemical properties of the fly ash are largely influenced by the chemical content of the coal burned (i.e., anthracite, bituminous, and lignite).

(a) Class F fly ash: The burning of harder, older anthracite and bituminous coal typically produces Class F fly ash. This fly ash is pozzolanic in nature, and contains less than 10% lime (CaO). Possessing pozzolanic properties, the glassy silica and alumina of Class F fly ash requires a cementing agent, such as Portland cement, quicklime, or hydrated lime, with the presence of water in order to react and produce cementitious compounds. Alternatively, the addition of a chemical activator such as sodium silicate (water glass) to a Class F ash can leads to the formation of a geopolymer.

(b) Class C fly ash: Fly ash produced from the burning of younger lignite or sub bituminous coal, in addition to having pozzolanic properties, also has some self-cementing properties. In the presence of water, Class C fly ash will harden and gain strength over time. Class C fly ash generally contains more than 20% lime (CaO). Unlike Class F, self-cementing Class C fly ash does not require an activator. Alkali and sulfate (SO_4) contents are generally higher in Class C fly ashes.

Present Scenario On Fly Ash In India

- Over 75% of the total installed power generation is coal-based
- 230 - 250 million MT coal is being used every year
- High ash contents varying from 30 to 50%
- More than 110 million MT of ash generated every year
- Ash generation likely to reach 170 million MT by 2010
- Presently 65,000 acres of land occupied by ash ponds
- Presently as per the Ministry Of Environment & Forest Figures, 30% of Ash
- Is being used in Fillings, embankments, construction, block & tiles, etc.

Rising energy costs and concerns about climate change due to indiscriminate use of fossil fuels would continue to drive advances in new technologies for harnessing renewable energy and energy efficient systems. It is an accepted fact that the buildings are not energy efficient and lot of scope exists to conserve energy by rendering buildings energy efficient.

Terrestrial solar radiation or sunlight, which reaches the ground, consists of three types of radiation; ultraviolet, visible and near infrared. While the ultraviolet portion of sunlight (280-400 nm) is ionizing radiation, the visible light (400-700 nm) is the colored portion. Near infrared region which typically extends from 700 nm to 2500 nm consists of maximum solar energy (~ 52%) **[1]**.

During summers in India, the temperature rises above 40^0C in many parts. The resultant heat build-up of roof and surface of buildings causes increased heat transfer into the building which results into increased cooling loads contributing to an increase in utility costs.

The coatings are applied to a surface to visually beautify and functionally protect the surface which may be metal wood or concrete. The pigments used for coating concrete structures can be made infrared reflective, which would not only impart color to an object but also reflect infrared portion of incident light or in other words heat and thereby minimizing heat build-up.

Cool coatings use pigments which reflect the incident sunlight and keep the objects cool. Pigment interactions with wavelengths outside the visible can have interesting effects on cooling properties. One key area of spectrum is the infrared (IR) region, specifically the near infrared (NIR) region. While not visible to human eye, a pigment and thus a coating's NIR reflective properties can affect its usability and durability.

The primary purpose of IR reflective coatings is to keep the objects cooler than they would be using standard pigments. This technology finds use in cool roofing, transportation etc. Significant work has been carried out in this area.
An infrared reflective material was developed which could be **[2]** applied directly to the bituminous surface of a roofing product to increase the solar reflectance of the product. Preparation of solar reflective granules having deep tone colors by coating base mineral particles with a coating composition including an IR reflective pigment is reported **[3]**. Tin doped indium oxide nanoparticles with the particle size in the range of 15-30 nm were successfully prepared by coprecipitation method and applied as NIR reflective film **[4]**. Ronnen Levinson et al reported work on non-white NIR reflective architectural coating which can be applied to in situ to pitched concrete or clay tile roofs to reduce tile temperature, building heat gain and cooling power demand while simultaneously

improving the roof's appearance. Scale model measurements of building temperature and heat flux were combined with solar and cooling energy use data to estimate the effects of such cool roof coatings in various California climates. It was observed that coatings reduced peak roof surface temperature by 5-14 K and peak ceiling heat flux by 13-21%. It was stated that the peak power demand reduction in cooler climates may eliminate the need to purchase an air conditioner **[5].**

An additional benefit of energy efficient coatings is their fire safety. It was reported by Paul Berdahl that coatings for improving energy efficiency of buildings have fire safety implications and vice-versa, because the emission spectrum of a fire overlaps at short wavelengths with the solar IR and overlaps at long wavelengths with 300 k thermal IR radiation **[6]**. Another much studied group of NIR reflective pigments is complex inorganic color pigments based on mixed metal oxides. The composites consisting of a coloring agent and a white pigment coated with another non- NIR absorbing pigment **[7,8]**. A review has been done by Ashwini K. Bendiganavale and Vinod C. Malshe on the NIR reflectivity of inorganic pigments. A comparative evaluation was done for the IR reflectivity of various commercially available pigments **[9]**. K.J. Sreeram et al prepared Ce-Pr-Mo and Ce-Pr-Fe pigments through appropriate doping to offer a reddish brown and reddish orange color respectively. These pigments with over 65% reflectance in the NIR region can well serve as cool colorants **[10]**.

Research Objectives:

In the present work, we have addressed two problems simultaneously, i.e. utilization of flyash as an IR reflective material in paints and development of NIR reflective coatings. The surface modification of flyash is done by coating it with metal oxide i.e. TiO_2 through a simple and economic process and then coatings were prepared by coating this material on the mild steel panels by spray coating technique. This work has led to development of energy efficient coatings based on industrial waste with an added

advantage of being antiabrasive and anticorrosive in nature and use of flyash as a filler material for EMI shielding applications

Methodology

Cleaning of Flyash:

1. Flyash collected from the power station was first treated to remove iron oxide and unburnt carbon.
2. The treated sample was then used in preparation of core shell composites by depositing nano titanium dioxide on treated flyash core by using different methods.

Removal of iron oxide particles

1. Fly ash was first graded to 2-25 µm size and then subjected to wet magnetic separation to remove magnetically active iron oxide particles.
2. For this, slurry was made by adding 1000 ml distilled water to 200 gm of graded flyash. The slurry was stirred well using a large bar magnet when magnetic iron oxide particles stick to it.
3. The magnet was taken out, washed and used again. This process was repeated until all magnetically active particles were removed from flyash.

Acid leaching for removal of non-magnetic iron oxide particles

1. This was followed by acid leaching wherein 100 ml of 10 M HCl was added to the slurry and heated to 50-60^{o}C for 2 hr. Non- magnetic iron oxide is removed by this process.
3. Fly ash is then washed till neutral pH. Unburnt carbon particles were removed by **ultrasonication.**
4. Flyash after treatment was analyzed for unburnt carbon and iron content.

Preparation of Core Shell composites

Core Shell composites were prepared using fly ash as a core and Titania as shell. Titanium isopropoxide was added dropwise into the solution containing fly ash.Flyash particles free of unburnt carbon and oxides of iron was used as core.

Method 1: Ex-situ Precipitation Method

Commercially available Titanium dioxide was subjected to ball- milling in iso-propanol medium using tungsten carbide balls. Ball Milling was continued for 4 hr at 200 rpm till nanosize was achieved which was confirmed by XRD analysis.

To prepare core shell by ex-situ method, treated Fly ash was mixed with ethanol solution and Sodium Oleate. The slurry was subjected to vigorous stirring for 1 hr. Ball milled TiO_2 was added to this mixture and again stirred vigorously for 2 hr. This was followed by ultrasonication for 2 hours. Solvent was then removed by drying at 50-60^oC for several hours. The powder obtained was then heated in a vacuum oven at 120^oC for 2 hours. Two samples of fly ash core composites were prepared by ex-situ method in which two different proportions of flyash and TiO_2 (1:1 and 1:2 respectively) were used.

Method 2: Insitu Precipitation Method- Solvent Based

Core Shell composites were prepared using fly ash as a core and Titania as shell. Surfactant solution was added in the solution containing flyash (0.5%, 1%) and then Titanium isopropoxide was added dropwise. The composite particles were then treated at 120^0, 600^0, 800^{0}C. Three coatings of TiO_2 on flyash was done by the above procedure and subjected to heat treatment. Similar procedure was repeated with zero surfactant concentration also.

Method 3: Aqueous method

It was done in two ways. Firstly, core shell particles were prepared by the addition of surfactant modified flyash in HCl solution followed by dropwise addition of Titanium

isopropoxide. The solution was then sonicated for one hour and then centrifuged, washed and dried. Composite particles were then subjected to heat treatment at 120^0, 600^0 and 800^0C. Two coatings of TiO_2 on flyash was done.

Alternatively, core shell particles were prepared by adding SCFA (single coating of TiO_2 on flyash) that was prepared by precipitation method in HCl solution followed by addition of Titanium isopropoxide. The solution was then sonicated, centrifuged, washed and dried. Composite particles treated at 120^0, 600^0, 800^0C. Two coatings of TiO_2 on flyash was done.

Method 4: Chemical modification of flyash

Flyash was fused with sodium hydroxide pellets at high temperature for 3 hours. The mixture was neutralized with water and then dried and finely grounded.

Application of coatings on steel panels:

The FA/TiO_2 core shell particles (5% w/w) prepared by different techniques were mixed with epoxy resin in a ball mill for 1 hr. Then spray coating was done on (33/33 mm) steel panels. The panels were dried at 120^0C in oven and the panels were then analyzed by UV-DRS technique to calculate its reflectivity and emissivity.

Coatings of chemically modified flyash were also prepared by similar procedure and then analyzed by UV-DRS technique.

Wet coating of single coated fly ash, Double coated flyash was also done with acrylic resin on the mild steel panels and the panels were analyzed.

CHARACTERIZATION:

Fly ash was characterized for its elemental composition and mineral phase composition by Energy Dispersive X-ray analysis (EDAX) and X-ray Diffraction (XRD) analysis

respectively. A Broker make D-8 ADVANCE powder X-ray diffractometer was used to identify the mineral phase composition of fly ash. CuKά radiation (λ= 1.5406 A^o) was used to record the patterns. All the patterns were recorded between 10-80^o. The cleaned fly ash sample was also analyzed using similar techniques to compare the content of iron oxide and unburnt carbon in treated and untreated fly ash samples. Morphological characteristics of flyash and its core shell composite particles were studied using SEM LEO-440 and HRTEM (JEOL 2100 F). To measure Near Infrared (NIR) reflectivity of core shell composite particles Diffused Reflectance Spectra was recorded using UV-VIS-NIR spectrophotometer (Perkin-Elmer Lambda-950). Solar reflective Index was calculated according to the ASTM standard E891-87. Whiteness Index of the coatings was measured using Novo- Shade DUO, 45^0/0 Opacity/ Shade Meter. Thickness of the coatings was measured using Positest DFT, Model: DFT-C

RESULTS & DISCUSSIONS:

Table 1: Elemental composition of untreated fly ash Energy Dispersive X-Ray Analysis (EDS), also referred to as EDX and EDAX, EDS is an x-ray technique used to identify the elemental composition of a specimen.

Elemental composition	**Element weight %**		**Atomic %**	
	Untreated flyash	**Treated Flyash**	**Untreated Flyash**	**Treated flyash**
C	0.83	0.11	0.48	**0.24**
O	51.58	56.84	65.93	**66.97**
Mg	0.63	0.57	0.56	**0.56**
Si	23.93	25.21	17.36	**17.16**
Al	17.41	15.30	13.95	**10.17**

Fe	4.20	0.14	1.60	**0.15**
Ca	**1.42**	**1.83**	**0.12**	**0.37**

Method 1: Ex-Situ Precipitation Method

Morphological Analysis of composite particles using SEM:

Fig. 2a shows the SEM of Treated Fly ash. Fig. 1b shows the SEM of FA/TiO_2 prepared by Ex-situ Precipitation Method. It can be clearly seen in Fig. 2 that TiO_2 particles do not coat on the Fly ash particles. Shell formation does not take place. TiO_2 particles are dispersed in surroundings. Thus, Ex-situ precipitation method was not appropriate for the formation of Core shell composite particles.

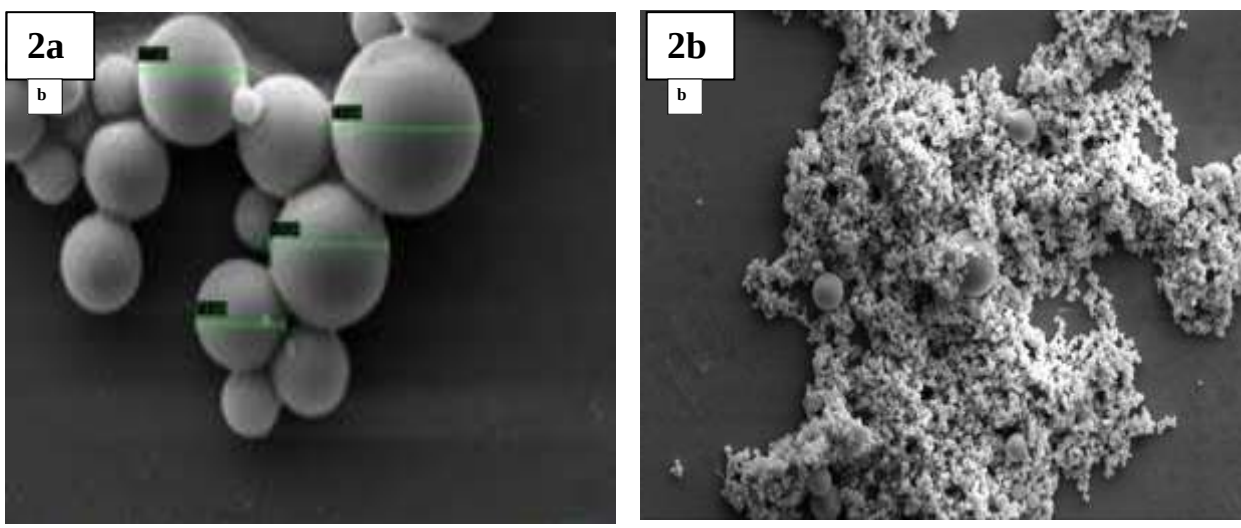

Fig. 2: SEM of (a) Treated Fly ash (b) FA/TiO_2 prepared by ex-situ precipitation method

Method 2: In-situ Precipitation Method- Solvent Based

Morphological Analysis of composite particles using SEM:

The SEM image of TiO_2 coated Fly ash in absence of surfactant is illustrated in Fig.3a. The TiO_2particles are not deposited on the Fly ash spheres but they are disseminated in

the surroundings as can be seen in photograph. Fig.3b shows the SEM images of TiO_2 coated Fly ash in presence of surfactant. It shows the homogeneous coating of TiO_2 on fly ash is achieved in this case. A smooth and uniform layer of TiO_2 can be seen on the Fly ash particle.

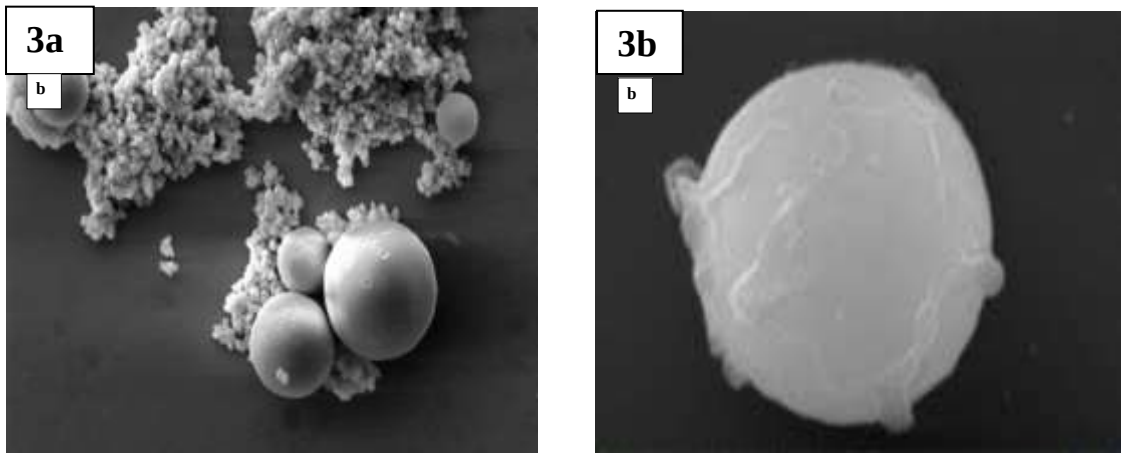

Fig. 3: SEM of FA/TiO_2 prepared by Insitu Precipitation Method (a) In absence of Surfactant (b) In presence of surfactant

Morphological Analysis of composite particles using TEM:

Selected core-shell composite samples were then chosen to confirm the formation of TiO_2 shell on Fly ash particles using TEM. Fig. 4a shows the morphology of the Uncoated Fly ash particles and Fig. 3b shows the morphology of TiO_2 coated Fly ash particles. It clearly shows that there is cloudy appearance around the Fly ash particles in Fig. 3b which is not present in uncoated fly ash particles as can be seen in Fig. 4a.Thus it can be predicted that TiO_2 shell is formed around Fly ash core in Fig. 4b.Fig. 4c shows uniform TiO_2 particle of 2-4 nm sizes obtained from TEM patterns The inter–grain connectivity of particle formation is a very clearly demarked by grain boundary process. The surface morphology of the particles shown in Fig. 4d can be indexed as a tetragonal anatase TiO_2 single crystal. The first rings are assigned to the (100) and second ring for (200), (211), (204) reflections of the anatase phase.

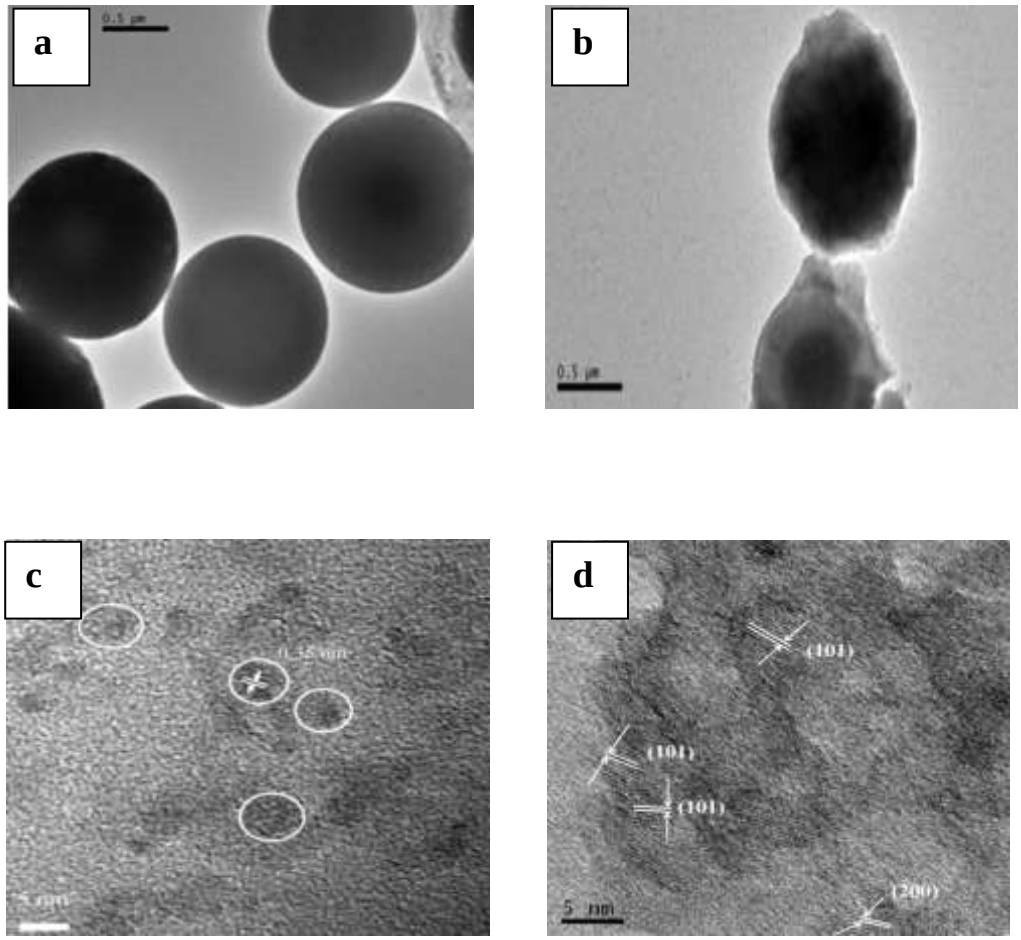

Fig. 4: TEM of (a) uncoated Fly ash (b) coated Fly ash (c&d) Lattice infringement of coated samples.

XRD Analysis:

Fig. 5b is the XRD patterns of TiO_2 coated fly ash according to different temperature of heat treatment. The crystalline structure of TiO_2 coated on fly ash shows a typical anatase and is well retained in the temperature range of 400-600^{0}C.The XRD pattern of SCFA and TCFA at 800^{0}C in Fig. 5a shows that conversion of anatase to rutile has started. The peaks corresponding to 101 plane and 200 plane of anatase TiO_2 appeared at 2θ = 25.4^0 and 48^0 respectively and the peaks of mullite of fly ash appeared at 2θ = 26^0 and 26.5^0.The peak of anatase was broader at lower temperature and this intensity increases with increasing the temperature. This result implies that crystallinity and crystallite size of anatase phase of TiO_2 coated Fly ash increases as temperature of heat

treatment increases. The peak corresponding to 110, 101 & 211 plane of rutile phase appeared at 2θ = 27^0, 36^0& 55^0 respectively when TiO_2 coated fly ash was treated at 800^0C. This result implies the conversion of anatase to rutile has started when temperature increases to 800^0C. The presence of anatase and rutile phases of TiO_2 was further confirmed by comparing with JCPDS standard files #21-1272 and #21-1276, respectively.

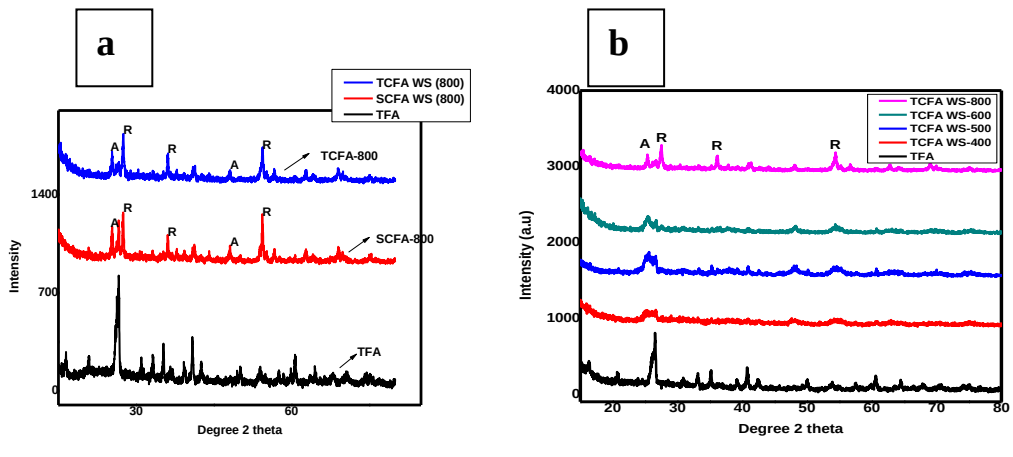

Fig. 5: XRD results: a)XRD diffraction pattern of TFA, SCFAWS-800 and TCFAWS-800 b) XRD diffraction pattern of raw flyash and triple coated flyash at different calcinations temperature

Raman Analysis:

Since XRD peaks are diffuse so Raman analysis was done to confirm the formation of anatase and rutile phase.

Raman analysis was undertaken in the range of 300-700 cm^{-1} as shown in Fig. 6. It can be seen in Raman spectra that in TCFA treated at 120^0C, there is appearance of anatase peaks at approximately 397 cm^{-1} (corresponding to B1g vibration mode), 516 cm^{-1} (A1g mode) and 640 cm^{-1} (Eg mode).

Also, from Raman spectroscopy, in addition to anatase the presence of second phase, rutile is also detected on annealing at 600^0C. The rutile phase first appears in sample annealed at 600^0C with a peak occurring at approximately 450 cm^{-1}(Eg mode) but its intensity is lower as rutile is just starting to form.

Raman peaks are not present in TCFA having zero surfactant concentration i.e. TCFA-0-120 but anatase peak starts appearing in TCFA-1-120 i.e. TCFA having 1% surfactant concentration and treated at 120^0C at approximately 639 cm^{-1}, 518 cm^{-1} and 398 cm^{-1} and the peaks become more intense with increase in temperature at 600^0C. The rutile peak is also detected at approximately 450 cm^{-1} with low intensity.

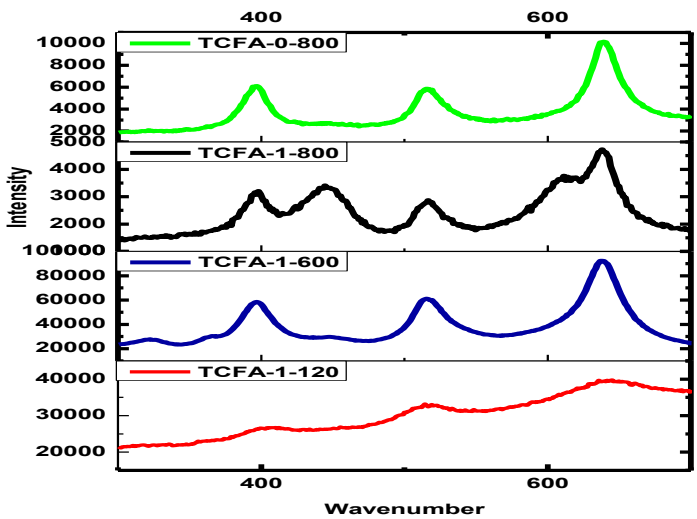

Fig. 6: Raman spectra of TCFA annealed at 120, 600 and 800 ^{0}C and TCFA having zero surfactant concentration and annealed at 120 & 800^0C

Solar Reflective Index of Powder and Coated samples:

Solar reflective index (SRI) is calculated using the solar reflectance (R*), thermal emittance and wind coefficient to ascertain efficacy of a cool pigment. ASTM E1980-01 method was used for calculating SRI. Materials having highest SRI values are preferred for cool coating applications. Table 2 indicates that TCFA WS-800 exhibits highest SRI value of 77 as compared other materials indicating it to be good NIR reflective materials.

TCFA WS-800 coated on steel panel shows highest SRI value of 92.04 as shown in Table 3.

Table 2: Solar Reflective Index of Powder Samples as per ASTM standard E 1980-01:

S.No.	Sample	Reflectance at R* (%)	Emittance	SRI value at R*
1.	UN-FA	48.2	0.85	54.0
2.	TFA	52.3	0.85	60.0
3.	SCFA WTS	55.2	0.86	64.0
4.	SCFA 0.5% WS	59.3	0.87	70.0
5.	SCFA 1% WS	60.0	0.85	71.0
6.	TCFA WS-120	64.1	0.85	76.0
7.	TCFA WS-800	64.9	0.88	77.0

Table 3: Solar reflective index of coatings on steel panels (ASTM Standard E 1980-01):

S.no.	**Sample**	**Reflectance**	**Emittance**	**SRI**
1.	Pure Epoxy	0.75	0.86	87.20
2.	TCFA 1% SD	0.60	0.85	70.58
3.	TCFA 600	0.80	0.87	91.95

4.	TCFA 800	0.81	0.88	92.04
5.	TFA	0.66	0.87	75.86
6.	Untreated FA	0.68	0.86	79.06

Diffuse Reflectance Spectra Analysis of Powder samples and coatings on steel panels:

Fig. 7a and 7b shows the diffused reflectance spectra of single and triple coating of TiO_2 on Fly ash powder samples and Fig. 7c and 7d shows the diffused reflectance spectra of single and triple coating of samples coated on steel panels respectively. Fig. 7b clearly indicates that TCFA WS- 800 is having highest reflectance as compared to TCFA WS& TCFA WS- 600. It shows that reflectance is increasing with increase in the annealing temperature as crystallinity of TCFA WS increases with increase in temperature which is evident from XRD as shown above. Same trend is followed in coated samples in Fig. 7c & 7d. TCFA WS-800 shows highest reflectivity.

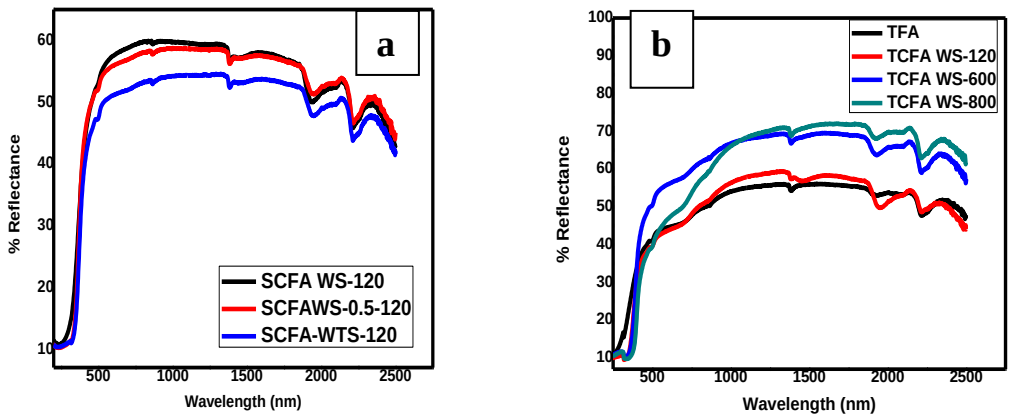

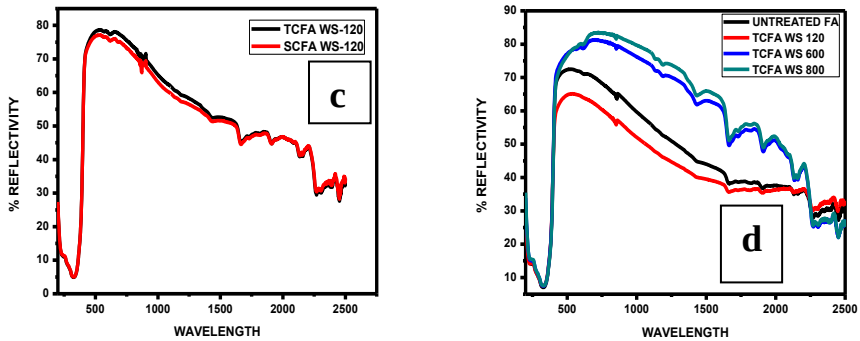

.

Fig. 7: DRS results of powder samples:a) Diffuse Reflectance Spectra of Single coated flyash in presence of different surfactant concentration and in absence of surfactant b) Diffuse Reflectance Spectra of Treated flyash and triple coated flyash annealed at different temperatures. c) Diffuse Reflectance Spectra of Single and triple coated flyash with TiO_2 coated on steel panels d) Diffuse Reflectance Spectra of triple coated flyash treated at different temperatures and untreated fly ash coated on steel panels.

Whiteness index of coatings on steel panels:

Whiteness Index of the pigments was measured using Novo- Shade DUO, 45^0/0 Opacity/ Shade Meter. The pigment was mixed with epoxy resin in different percentage (5%, 10%, 15%) by ball milling for 2 hours. It was noticed that thickness of panel increases with increase in the pigment concentration in the epoxy resin which was measured using Positest DFT, Model: DFT-C. Also whiteness index increase with the increase in the pigment percentage and thickness except in the case of untreated flyashand treated fly ash because darkness increases with increase in percentage of pigment concentration in epoxy resin.

Table 4: Whiteness index of coatings on steel panels:

S.No.	Sample	Percentage (%)	Thickness	Whiteness Index
1.	UnFA= Untreated	5	55	65.9

	Flyash			
		10	66	63.7
		15	74	61.5
2.	TFA	5	48	49.5
		10	51	60.5
		15	63	70.2
3.	TFA -500	5	60	64.7
		10	72	65.9
		15	92	67.1
4.	TiCOM	5	98	72.7
		10	115	73.4
		15	212	80.67
5.	Pure epoxy	5	82	85.1
6.	SCFA 1% WS	5	60	66.3
		10	74	66.7
		15	96	78.9
7.	TCFA 1% WS	5	70	66.7
		10	72	76.9
		15	96	79.8

8.	TCFA WS-600	5	86	71.2
		10	130	76.2
		15	157	76.8
9.	TCFA WS-800	5	48	61.2
		10	58	62.3
		15	102	78.7

Method 3: Aqueous Method

Morphological Analysis of composite particles using SEM:

The SEM image of TiO_2 coated Fly ash by aqueous method I is illustrated in Fig.8a & 8b. Uniform coating of TiO_2 particles can be clearly seen on the Fly ash particles. The SEM image of TiO_2 coated Fly ash by aqueous method II is illustrated in Fig.8c & 8d. It is also showing the homogeneous coating of TiO_2 on fly ash spheres.

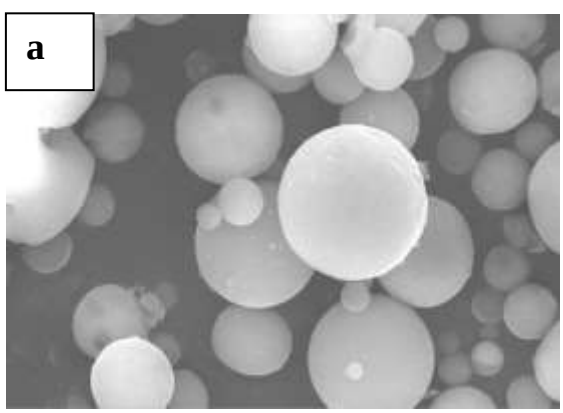

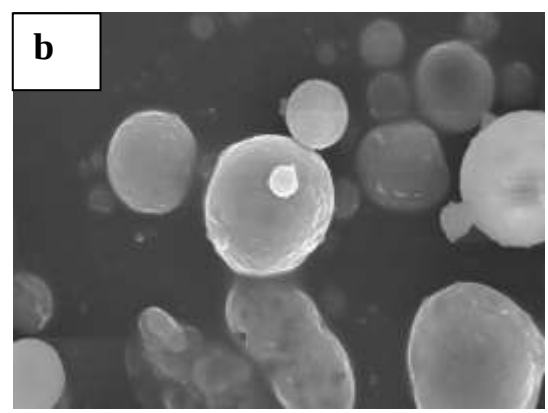

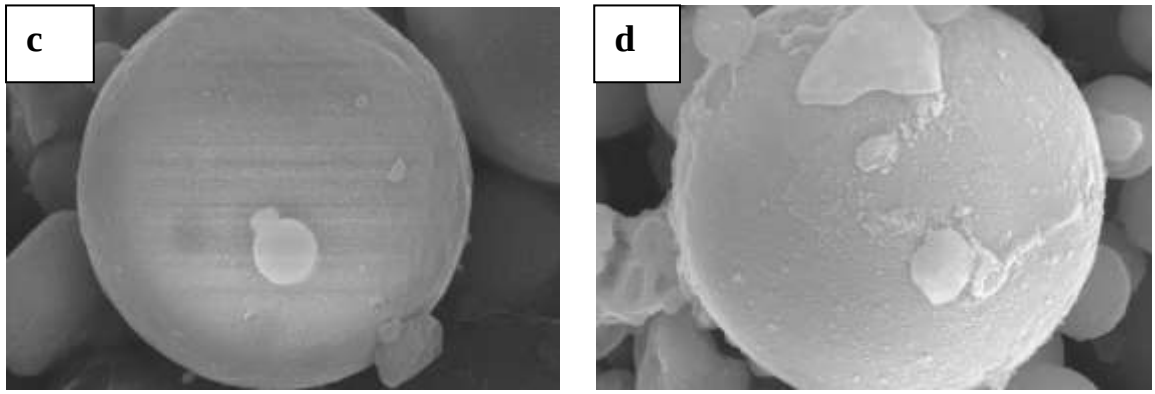

Fig. 8: (a&b) SEM of FA/TiO_2 prepared by aqueous method (Method 1): (Single and double coating) (FA-UT-MF and FA-UT-MF-DC) (c&d) SEM of FA/TiO_2 prepared by aqueous method (Method 2): (Single and double coating) (SCFA- UT and SCFA-UT-DC)

Diffuse Reflectance Spectra Analysis of powder samples and coated samples:

Fig. 9a and Fig. 9b shows the diffused reflectance spectra of TiO_2 coating on Fly ashprepared by aqueous method I and method II respectively. Fig. 9c and Fig. 9d shows diffused reflectance spectra of samples coated on steel panels. Double coating of TiO_2 on fly ash prepared by both the methods is having highest reflectance as compared to single coatings of TiO_2 on Fly ash prepared by method 1 & method 2.

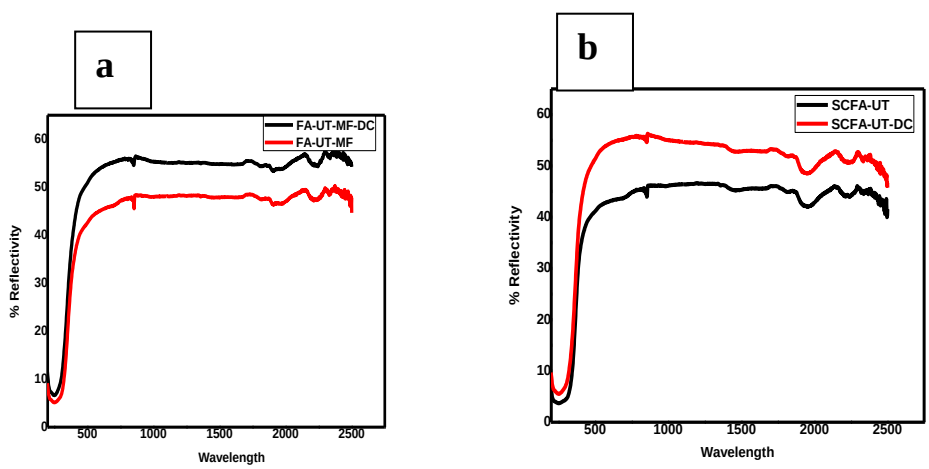

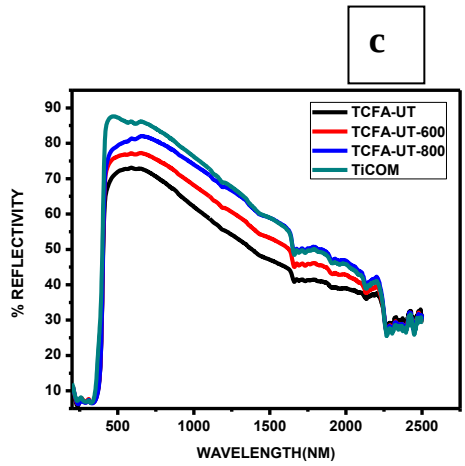

Fig. 9: Diffuse Reflectance Spectra of a) FA/TiO_2 powder prepared by aqueous method Ib**)** FA/TiO_2 powder prepared by aqueous method II c**)** Triple coated flyash treated at different temperatures prepared by aqueous Method Id)Triple coated flyash treated at

Table 5: Solar reflective index of powder samples (ASTM Standard E 1980-01):

S.No.	Sample	Reflectance at R* (%)	Emittance	SRI value at R*
1.	UN-FA	48.2	0.85	54.0
2.	TFA	52.3	0.85	60.0
3.	FA-UT-MF	67.83	0.93	82
4.	FA-UT-MF-DC	75.44	0.87	92
5.	SCFA-UT	65.60	0.87	78
6.	SCFA-UT-DC	74.62	0.90	91

different temperatures prepared by Aqueous Method II.

Solar Reflective Index of Powder samples:

Table 5 indicates that TiO_2 coated flyash prepared by aqueous method I exhibits highest SRI value of 92 as compared other materials indicating it to be good NIR reflective materials.

Method 4: Chemical Modification of Fly Ash

Morphological Analysis of composite particles using SEM:

Fig. 10 a and 10 b shows the complete conversion of fly ash into amorphous alumino silicate at low magnification and high magnification respectively.

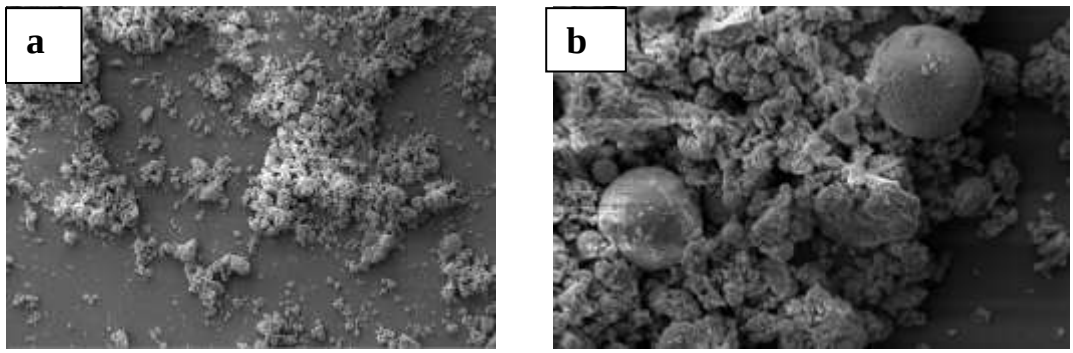

Fig. 10: (a) SEM Image of Chemically Modified Fly ash (CMFA) - Low magnification (b) SEM Image of Chemically Modified Fly ash (CMFA)-High magnification

Diffuse Reflectance Spectra of Chemically modified fly ash (CMFA):

Fig. 11a and Fig. 11b shows the Diffused Reflectance spectra of chemically modified fly ash powder and coated on steel panels. CMFA is showing good reflectivity of almost 80% in coated sample.

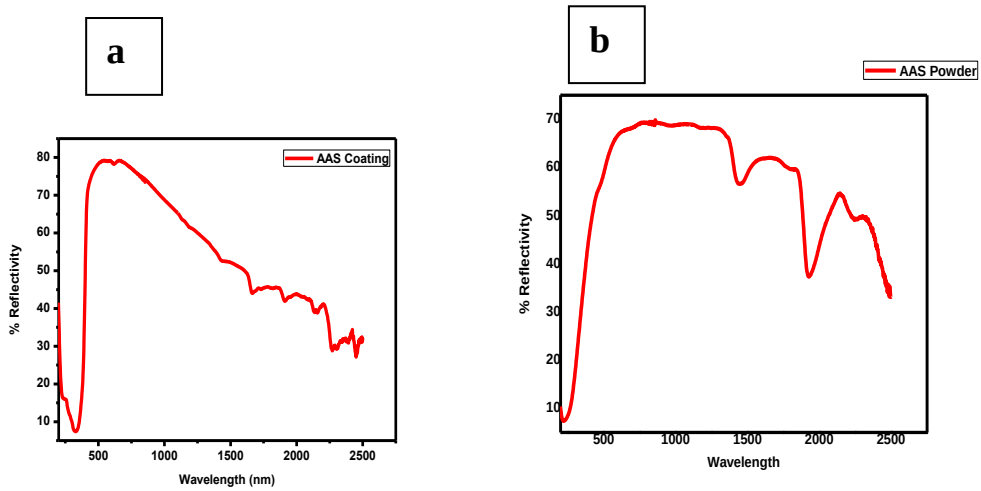

Fig. 11: (a) Diffuse Reflectance Spectra of chemically modified flyash Powder sample (b) Diffuse Reflectance Spectra of chemically modified flyash coated on steel panel

Conclusion:

TiO_2 coated Fly ash composite particles prepared using In-situ Precipitation - solvent based method and Aqueous method shows promising results making them potential candidate for using it in a cool pigment. But the core-shell composites prepared by using Aqueous method has advantages over In-situ Precipitation - solvent based method as it is solvent free method hence environmental friendly. The difficulty in dispersion of Fly ash during coating process was solved in aqueous method where it was dispersed through ultra-sonication and therefore more uniform coating of TiO_2 on Fly ash was obtained.

In the second part of the chapter, studies were carried out to explore the utilization of fly-ash composites for shielding of electromagnetic radiations in X-band and Ku-band and for designing these composites for dissipation of electrostatic charge.

Besides electromagnetic radiation pollution and electrostatic charge dissipation, our society is also dealing with a number of other serious environmental issues such as solid waste/ air pollution. Disposal of solid waste/ by-products, generated from various industries is a growing concern to reduce landfills. Fly ash is a major combustion residue, produced from the coal burning in the thermal power stations. The composition and

properties of these solid by-products dependents on the coal types and technological processes used in thermal power stations. Besides being a solid waste fly ash offers few precious properties, such as low density, strong filling ability, excellent fluidity, chemical inertness, thermal resistance and being an inactive inorganic host without redox character, the incorporation in flexible foam matrix can be easily controlled. Depending upon the source and makeup of the coal being burned, the components of the fly ash produced vary considerably, but all fly ash includes substantial amounts of silica (silicon dioxide, SiO_2) (both amorphous and crystalline) and lime (calcium oxide, CaO). In general, fly ash consists of SiO_2, Al_2O_3, Fe_2O_3 as major constituents and oxides of Mg, Ca, Na, K etc. as minor constituent. Fly ash particles are mostly spherical in shape and range from less than 1 µm to 100 µm with a specific surface area, typically between 250 and 600 m^2/kg. The specific gravity of fly ash vary in the range of 0.6-2.8 gm/cc. Physical properties of fly ash mainly depend on the type of coal burned and the burning conditions. Class F fly ash is generally produced from burning high rank (containing high carbon content) coals such as anthracite and bituminous coals, whereas, Class C fly ash is produced from low rank coals. Fly ash particles are classified into two types, precipitator and cenosphere. Generally, the solid spherical particles of fly ash are called precipitator fly ash and the hollow particles of fly ash with density less than 1.0 g cm^{-3} are called cenosphere fly ash. One common type of fly ash is generally composed of the crystalline compounds such as quartz, mullite and hematite, glassy compound such as silica glass, and other oxides. The precipitator fly ash, which has a density in the range 2.0–2.5 g cm^{-3} can improve various properties of selected matrix materials, including stiffness, strength, and wear resistance and reduce the density. Cenosphere fly ash, which consists of hollow fly ash particles, can be used for the synthesis of ultra-light composite materials due to its significantly low density, which is in the range 0.4–0.7 g cm^{-3}, compared with the densities of metal matrices, which is in the range of 1.6–11.0 g cm^{-3}. Coal fly ash has many uses including as a cement additive, in masonry blocks, as a concrete admixture, as a material in lightweight alloys, as a concrete aggregate, in flowable fill materials, in roadway/runway construction, in structural fill materials, as

roofing granules, and in grouting. The largest application of fly ash is in the cement and concrete industry, though, creative new uses for fly ash are being actively sought like use of fly ash for the fabrication of MMCs.

Effect on Electromagnetic radiations on Human health

Several studies shows environmental exposures to EMF can interact with fundamental biological processes in the human body. This adverse effect can be short term or long term like increase in blood pressure, rise in body temperature and stress etc. Indian Council of Medical research (ICMR) has indicated that the hot tropical climate of the country, low body mass index (BMI), low fat content of an average Indian as compared to European countries and high environmental concentration of radio frequency radiation may place Indians under risk of radio frequency radiation adverse effect. So disclosure to EM waves can cause diseases like fatigue, sleep disturbance, dizziness, lack of concentration, ringing in the ears, reaction time, loss of memory, headache, disturbance in digestive system, cancer, sperm dysfunction and heart palpitation etc.

Effect on Environment

In last decade electromagnetic pollution gain attention and several studies shows its effect on environment. Some studies suggest that disappearance butterflies, bees,

insects and sparrows from our surroundings are due to increase in mobile phone towers. To assess the effect of escalation of mobile tower in Urban, Sub-urban and even rural/forest area on the population of birds and bees, The Ministry of Environment & Forests, (Wild Life Division) has constituted a committee on 30th August 2010.Gavin.etal demonstrate that the sparrow exposed to EMI wave losses its navigational ability and fly in different direction.

Ministry notification

- For the past few months ago, mobile phone tower radiation was issue of the news. Recently new radiation norms were adopted by India and the Department of Tele communication (DoT) had set September 1, 2013 as the deadline for the telecom operators to adhere to them. As per the new norms, the operators were mandated to reduce the radiation levels by 1/10th of the current levels, thus making it 0.9 watt/m^2. Furthermore, it was announced that operators who are found flouting these rules would be heavily penalised.

How this problem can be solved by designing Flyash composites?

The present work relates to the preparation of flyash in the form of tiles by embedding specific filler materials which can be used for antistatic and EMI shielding applications.

More particularly the work relates to modification of fly-ash by adding fillers so as to achieve strength and should have electrical conductivity which makes it suitable for antistatic tiles and for EMI shielding applications which is the novelty of the work.

Surface Morphology and micro-structural analysis

The schematic representation of fly-ash incorporated with ferrofluid nanoparticles in the presence of MWCNT is shown in scheme 1.

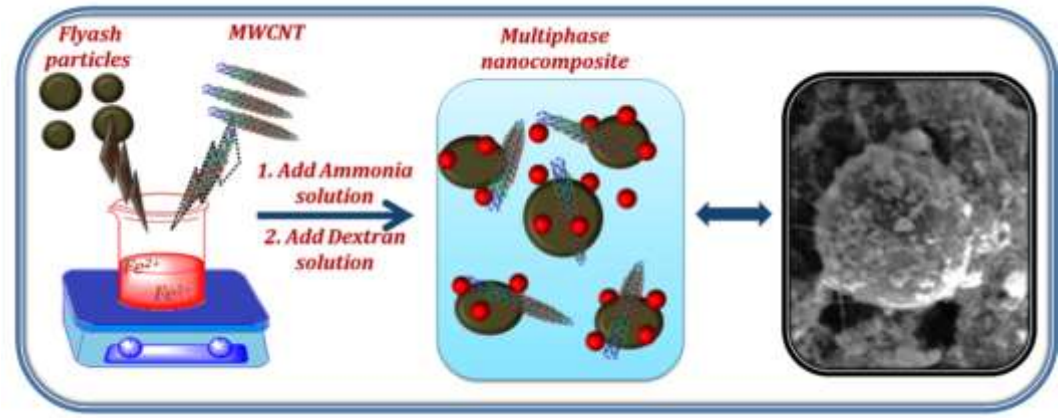

Scheme 1: Schematic representation of flyash particles surrounded with ferrofluid nanoparticles along with MWCNT'S by *in-situ* co-precipitation

SEM was carried out to study the distribution of fly-ash and MWCNT in the ferrofluid matrix. Fig. 12 (a) shows the SEM image of flyash particles up to a few micrometer in diameter, since flyash is composed of different oxides like SiO_2, Al_2O_3, CaO, K_2O therefore the different size spheres (diameter ranges from 50 nm - 5 µm) were seen in the SEM images. Fig. 12(b) shows high aspect ratio MWCNTs. SEM micrograph of MPC3 composites reveals that flyash particles are partially covered with ferrofluid nanoparticles along with MWCNT as appear in Fig. 12 (c) and Fig. 12 (d). The presence of conducting and the dielectric nanoparticles in the ferrofluid matrix is helpful for the

proper impedance matching, which is necessary for enhancing the absorption of the EM wave.

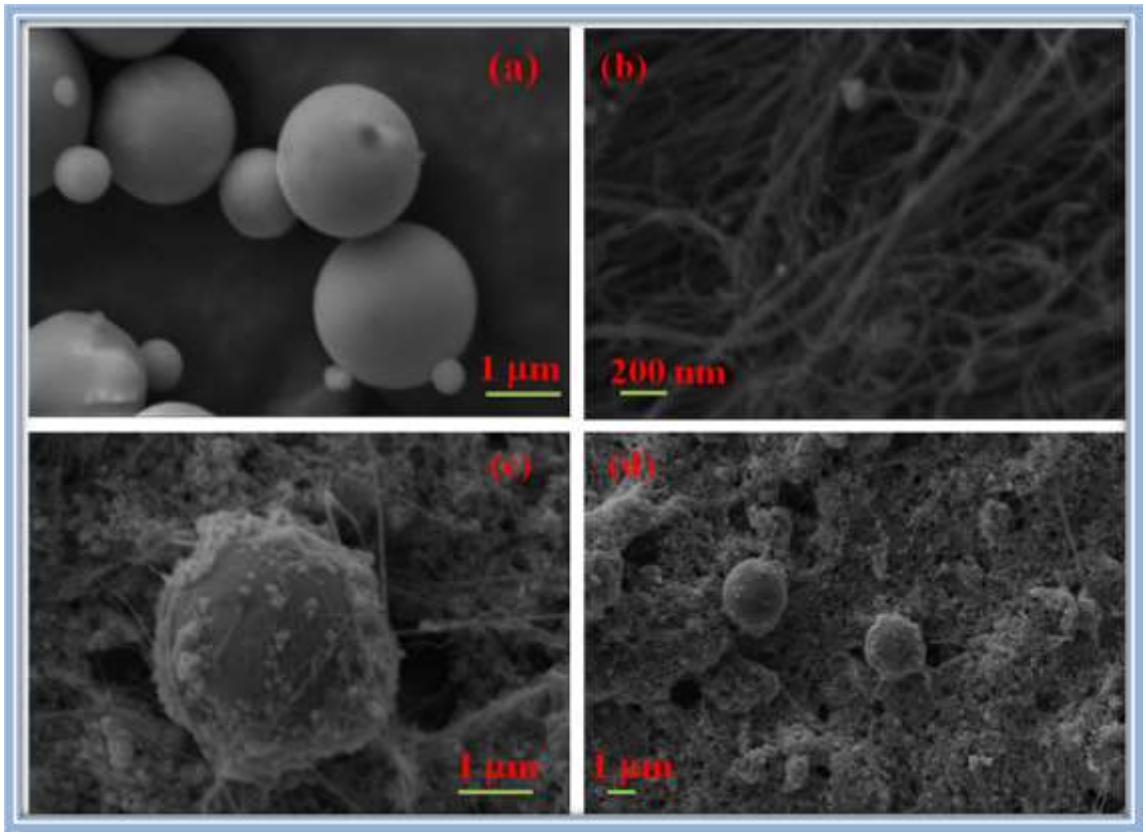

Fig. 12 SEM images of (a) fly-ash micro-particles (b) MWCNT (c) and (d) MPC3 composite, showing fly-ash particle coated with ferrofluid particle along MWCNT

TEM image of multiphase composite (MPC1) (Fig. 13 (a)) shows uniform distributed MWCNT, flyash particles covered with ferrofluid nanoparticles. The arrow shows the MWCNT and micro-flyash particle covered with ferrofluid is encircled. Fig. 13 (b) shows EDS pattern of flyash, the approximate percentage of the constituents of flyash like SiO_2, Al_2O_3, K_2O, and CaO etc. while Fig. 13 (c) shows the EDS pattern of multiphase composites (MPC1), there is a increase in the content of Fe & Carbon weight % in multiphase composites as compare to neat flyash.

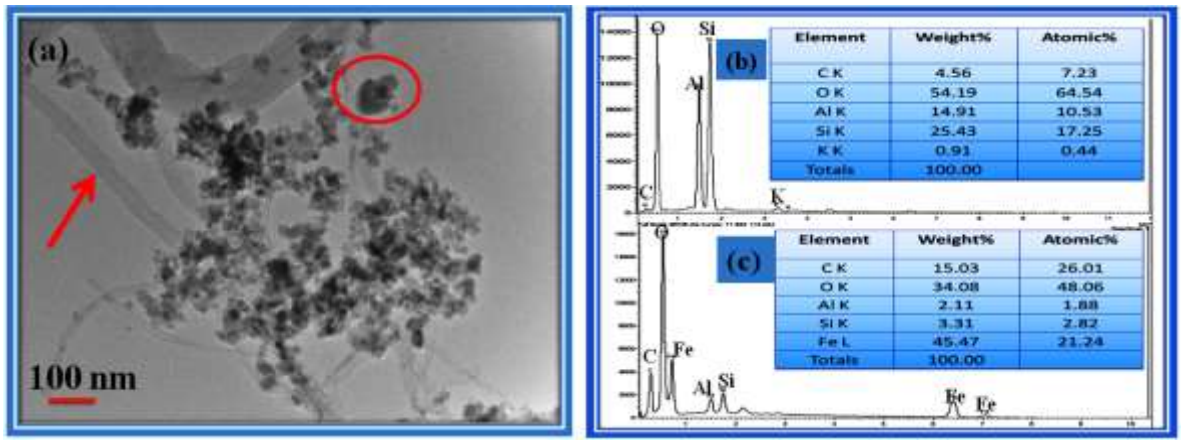

Fig. 13 (a) TEM image of MPC1 composite, EDS pattern of (b) flyash micro-particles (c) MPC1 composite.

Structural analysis

Fig. 14(a) shows the XRD patterns of pure MWCNT, flyash, ferrofluid and multiphase composites i.e.MPC1, MPC2, MPC3. Fly-ash shows the characteristics peaks at 2 θ = 26.68° (d = 3.3409 Å), 33.36° (d = 2.6931 Å), 35.22° (d = 2.5433 Å), 39.88° (d = 2.2057 Å), 42.46° (d = 2.1196 Å), 54.04° (d = 1.6955 Å), 60.68° (d = 1.5249 Å) and 64.60° (d = 1.4435 Å).The XRD patterns of MWCNT shows reflection peaks at 2θ values of 26.5°, 42.64°,corresponding to (0 0 2) (1 0 0), sets of diffraction planes, respectively. XRD pattern of Fe_3O_4 shows a main peaks at 2 θ values of 30.16° (d = 2.96 Å), 35.53° (d = 2.53 Å), 43.18° (d = 2.09 Å), 57.11° (d = 1.61 Å) and 62.71° (d = 1.48 Å) which corresponds to the (2 2 0), (3 1 1), (4 0 0), (5 1 1) and (4 4 0) reflection planes which matches with the standard XRD pattern of Fe_3O_4 (Powder Diffraction File, JCPDS card No. 88-0315). The composites show the characteristics peaks of MWCNT, flyash and ferrofluid, their intensity increases monotonically with increase in the content. It is seen that all the detectable peaks of flyash and ferrofluid are well retained and no other peak is observed indicating that no chemical reaction occurred between MWCNT, ferrofluid and flyash. These observations indicate that there is no change in the morphology of flyash, although it was coated by ferrofluid particles.

The crystalline size of particles can be calculated by using Debye Scherer's formula

$$D = k\lambda / \beta \cos\theta$$

where k is the Scherrer constant and equals 0.89, which is governed by several factors, including the Miller index of the reflecting plane and the shape of the crystal. is the X-ray wavelength, θ is the angle of the Bragg diffraction, and β is the full width at half-maximum of the sample. D is crystalline size for individual peak. The average size of Fe_3O_4 particles was calculated using above equation and estimated as 10.6 nm for pure Fe_3O_4 and 11.3 nm for Fe_3O_4 nanoparticles presented in multiphase composites.

FTIR spectroscopy

Fig. 14 (b) shows FTIR spectra of pure Fly ash, ferrofluid, and its composites. Fly ash spectra show a wide band which is a characteristic of the internal vibrations in silicates. The band corresponding to asymmetric stretching vibration of T-O (T = Al, Si) in the fly ash appears at 1083.90 cm^{-1}. Bands at 457.45 cm^{-1} are assigned to T-O bending vibrations. The bands at 780-795 cm^{-1} are attributed to the presence of quartz in the fly ash. The band at 550-560 cm^{-1} corresponds to the mullite present in the fly ash. Ferrofluid spectra show bending vibration of Fe-O, O-H at 582 cm^{-1} and 1620 cm^{-1} .The broad band observed around 3380-3430 cm^{-1} is due to the O-H stretching vibrations. These results are in good agreement with the previous spectroscopic characterization of ferrofluid. However, in case of composites, shows the characteristics band of ferrofluid and flyash indicating that flyash particles covered with ferrofluid also confirmed by SEM image (Fig. 13c). There is slight shifting and broadening of characteristics bands was observed which indicates the presence of physical interaction between MWCNT, ferrofluid and flyash. Absence of any new vibration band suggests a Vander Wall's kind of interaction without any chemical origin.

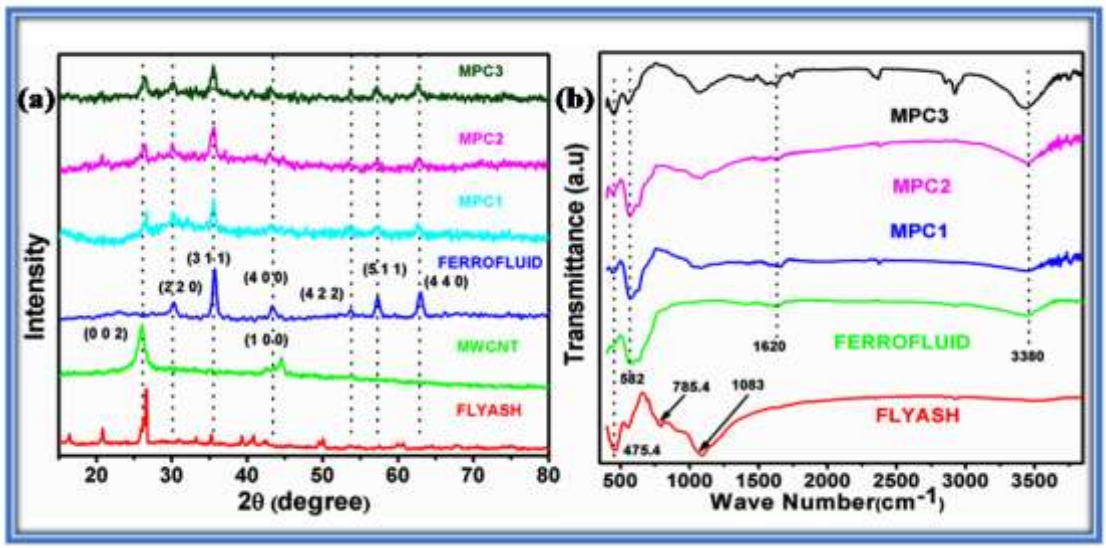

Fig. 14(a) XRD pattern of fly ash, MWCNTs, ferrofluid, MPC1, MPC2 and MPC3, (b) comparison of FTIR spectra of fly ash, FERROFLUID, MPC1, MPC2 and MPC3

Dielectric and Magnetic properties of multiphase composites

Fig. 15 (a) shows the real and imaginary part of complex permittivity and permeability for sample MPC3, as a function of frequency. The real part of permittivity (ε') symbolizes the intensity of polarization and it is a direct measure of the electrical energy storage ability of a material and permittivity loss represents the energy loss during the activation by an EM wave. The value of ε' fluctuates between 148 and 190. The value of ε'' is lower than ε' and it varies from 74 to 93 with fluctuations in 12.4 to 18 GHz. The high value of ε'' for multiphase composite exhibits high dielectric losses. Interestingly, there are two humps observed in dielectric loss which proposed that the two main phenomena's are responsible for dielectric losses. These may be interfacial polarization between fly-ash particles and MWCNTs, ferrofluid and MWCNTs and high anisotropy energy of the multiphase composite. Anisotropy energy of the small size materials like ferrofluid nanoparticles, would be higher due to surface anisotropic field due to the small size effect.[19] The higher anisotropy energy also contributes in the enhancement of the microwave absorption. The real part of

permeability (μ') varies from 1.17 to 0.63 while the imaginary part (μ'') i.e. permeability loss varies from 0.45 to 0.18. The fluctuations in the permeability curves reveals natural resonances in the multiphase composite which can be ascribed to small size of Fe_3O_4 nanoparticles. The both dielectric and magnetic losses share the improved shielding performance of the as-synthesized multiphase composites.

To further understand the magnetic behavior of the multiphase composites, the magnetic properties of the MWCNT/ferrofluid/flyash composites have been explored using the M–H curve (Fig. 15b). When MWCNTs are incorporated in the ferrofluid matrix with flyash in different weight ratio (i.e. 1:2:1 MPC1), the magnetization saturation (Ms) value has been found 38.26 $emug^{-1}$ at an external field of 5 kOe having small value of coercivity and negligible retentivity with no hysteresis loop, representing the super paramagnetic nature. However, on changing the weight composition of MWCNT/ferrofluid/flyash to 1:2:2, the Ms value has been decreased from 38.26 to 35.50 $emug^{-1}$, keeping the external applied field at 5 kOe. Ms value further decrease to 31.10 $emug^{-1}$ on changing the weight composition of MWCNT/ferrofluid/flyash to 1:2:3.In all the cases very small coercivity is observed with negligible retentivity which indicates the ferromagnetic nature. Decrease in Ms value is due to increase in the content of dielectric material in MPC composite matrix.

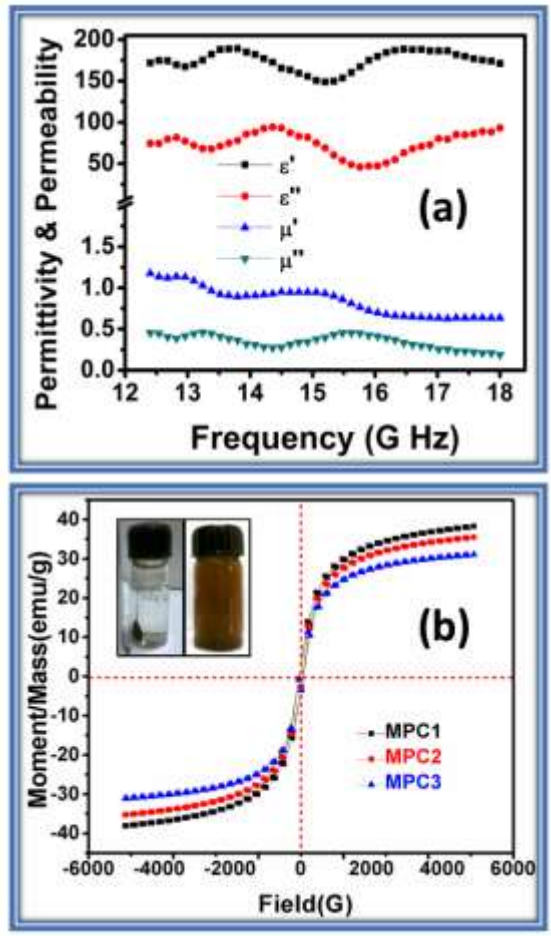

Fig.15. (a) Shows frequency dependence of the real parts and imaginary parts of the complex permittivity and permeability of Multiphase composites, (b) shows vibrating sample magnetometer plots of the Multiphase composites while Inset image shows the magnetic behavior of multiphase composite in presence and absence of bar magnet.

EMI shielding Efficiencies of multiphase composites

From the basic theory of EMI shielding, an ideal microwave shield must be a multiphase composite which contains the optimum concentration of electrically conducting material, dielectric filler and magnetic material. Along with this, physical geometry also plays crucial role in improving the SE. Moderate conductivity (10^{-4} to 10^{-1} S/cm) of the composite improves SE in two ways, first, incident EM wave reflected from the front face of conducting shield because interaction of electric vector with mobile charge carriers present on conducting surface resulted in ohmic losses (heat). Second, for

materials consisting of a high concentration of charge carriers (i.e., with a high conductivity), polarization due to the migration of charge carriers to form space charges at interfaces or grain boundaries becomes important. This space charge polarization enhances the polarization effect.

Being highly magnetic, conductive and high dielectric, flyash/ferrofluid/MWCNTs composites are an ideal material for EMI shielding to block polluting radiation in electronic gadgets. Certainly, MWCNTs and ferrofluid are counted for unprecedented EMI SE of flyash. The multiphase composites delivered exceptional EMI SE as high as about 48 dB at 25 wt% loading of flyash (Figure 16a), The SE decreased with increasing flyash loading in multiphase composite and reached a value of 38 dB at 50 wt% loading which is more than sufficient SE value required for commercial applications. The decreased in SE value with higher flyash loading can be attributed to two reasons, first incorporation of flyash leads to significant decrease in conductivity of multiphase composite as shown in table 1, second higher wt % of dielectric filler flyash raises the permittivity and lowering the equality of impedance matching i.e. $\varepsilon_r > \mu_r$. Figure 16 b shows the variation of SE due to absorption (SE_{Abs}) and due to reflection (SE_{Ref}) over the Ku band frequency range. Both SE_{Abs} and SE_{Ref} are collectively contributing to the total effective SE. The value of SE_{Abs} for MPC1, MPC2 and MPC3 were found to be ~40, ~36 and ~30 dB, respectively while the value of SE_{Ref} for all the composites is nearly same ~7dB. This is similar to the previous results i.e. SE_{Abs} becomes more dominant as compared to the SE_{Ref} in the microwave range. From these results, it is concluded that total SE is mainly dominated by SE_{Abs} while the SE_{Ref} is constant. Bare fly-ash shows a SE value of ~2.5 dB in Ku band (see supporting information). Therefore, it is worthy to notice that, total SE for all multiphase composites is multifold of bare fly-ash. For a given fly-ash content, all multiphase composites showed little fluctuation over the entire frequency range studied. The above observation is associated with three exceptional features of the multiphase composites: explicitly, (i) the presence of dielectric constituents in fly-ash contributed positively to shielding the electromagnetic waves (ii) ferrofluid nanoparticles act as tiny dipoles which get polarized by the activation of EM

field and result in better microwave absorption and (iii) the highly conductive MWCNT/ferrofluid/flyash multiphase composites had high charge storage capacities, capable of absorbing the incidental EM waves by polarization in the electric field. Besides these phenomena's, when EM waves incident on the material, ionic, electronic, orientational and space charge polarization occurs. The contribution to the space charge polarization appears due to the heterogeneous property of the material. From the all above, the result promises that these composites could be potentially used as a kind of radar absorbing material.

Table 6. The dc electrical conductivity and shielding effectiveness of multiphase composites

Sample Name	Conductivity (S/cm^{-1})	Shielding Effectiveness(dB)		
		SE_A	SE_R	SE_T
MPC1	38.56	~41	7.19	~48
MPC2	22.10	~36	8.22	~44
MPC3	10.49	~30	7.35	~37

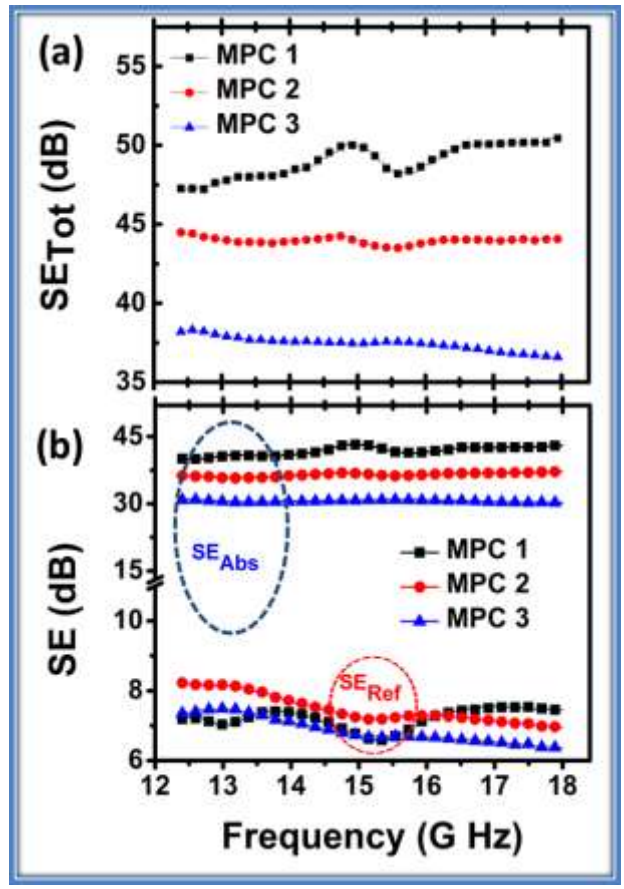

Fig.16. (a) EMI SE (b) SE_A and SE_R of multiphase composite as a function of frequency.

Multiphase composites consists of flyash, ferrofluid and MWCNTs have been prepared for efficient microwave shielding with different composition by utilizing the fly ash a waste material from various industries. This composition has been optimized and found MPC1 (1:2:1) better microwave shielding material where 48 dB of EMI shielding achieved in 12.4-18 GHz frequency (Ku band). The possible shielding mechanism of multiphase fly-ash/ferrofluid composites is shown in Fig. 17. The shielding effectiveness was strongly dependent on dielectric loss and volume fraction of in FA matrix. The high value of shielding effectiveness demonstrates the potential of these advanced multiphase composite as futuristic microwave shielding materials.

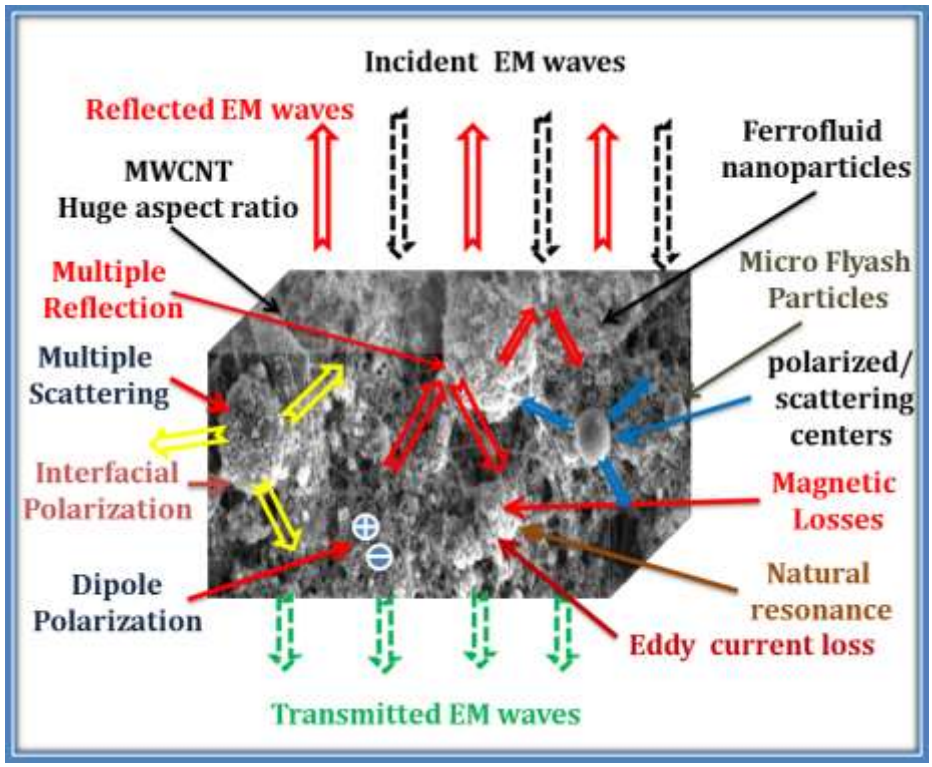

Fig.17. Possible shielding mechanism of multiphase composites.

Electromagnetic flexible foam by incorporating flyash

Consequently, we have studied another property of waste fly ash which has been utilized as filler in poly urethane foam matrix alongwith ferrofluid and activated charcoal so that the resultant flexible foam can be used for ESD and magnetic foam for pain relief therapy. The schematic representation of incorporation of flyash in ferrofluid matrix and incorporating it in the polyol and 2,4-toluene diisocyanate in the presence of catalyst and blowing agent is shown in Figure 18.

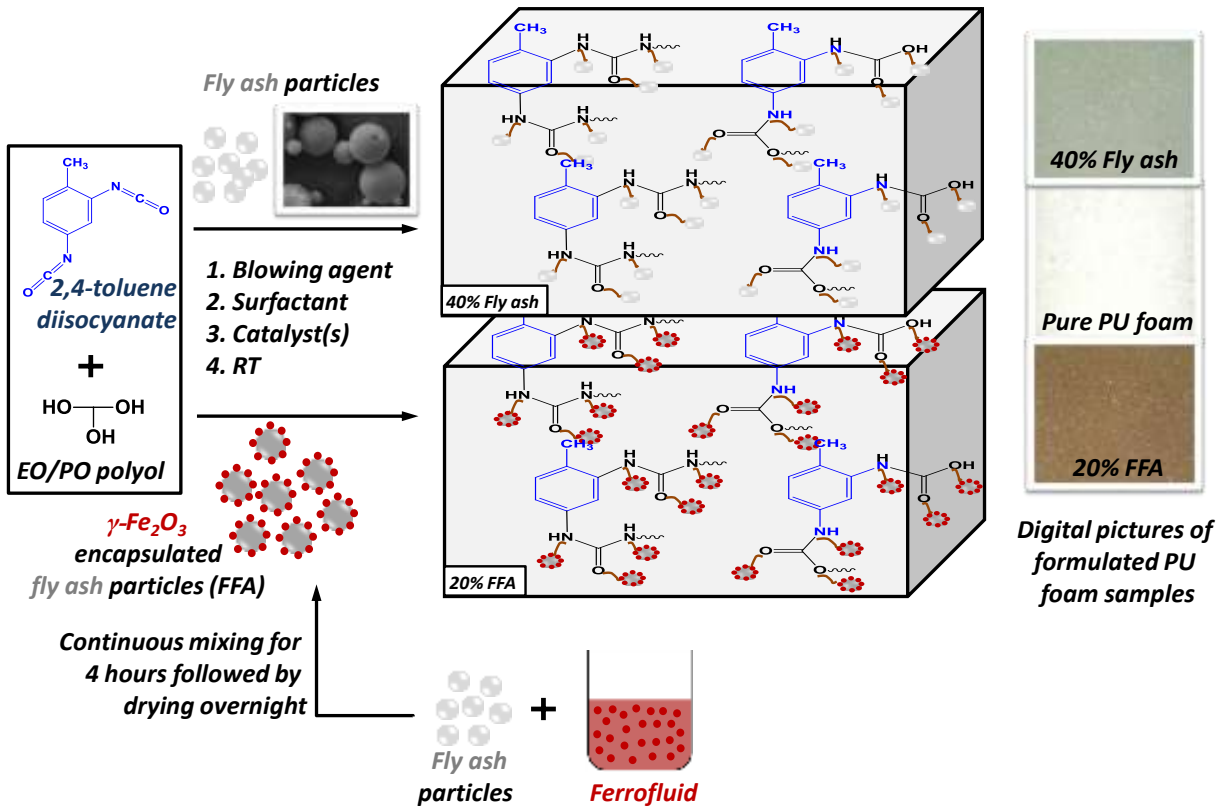

Figure 18: Schematic representation of formation of flexible foam incorporated with fly-ash and ferrofluid

SEM micrographs of designed polyurethane foam and the PU foam incorporated with fly-ash and ferrite particles is shown in Fig. 19

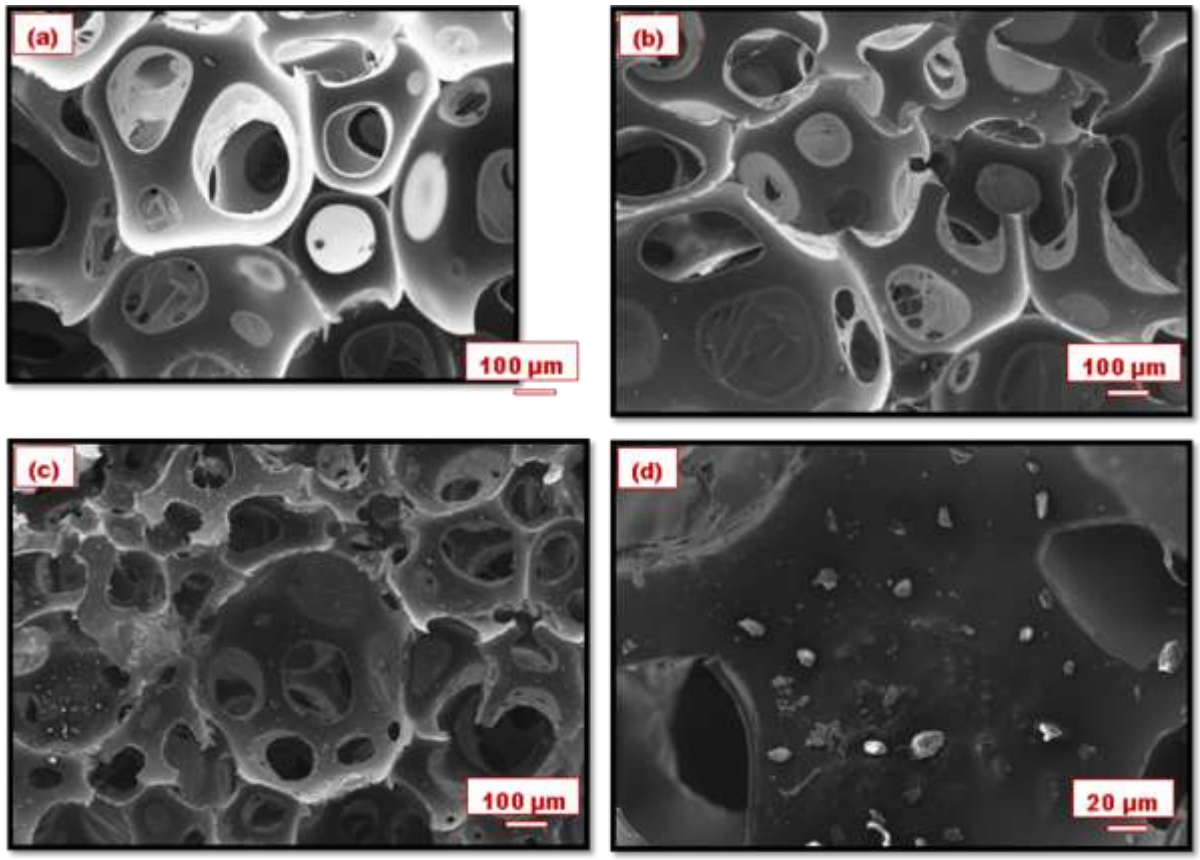

Fig.19 SEM micrographs of **a)** Reference polyurethane (PU) foam, PU foam with **b)** fly-ash, **c)** & **d)** Fe_2O_3 encapsulated on fly-ash

The flow chart for the preparation of polyurethane foam with flyash and ferrofluid is shown in Fig. 19 A.

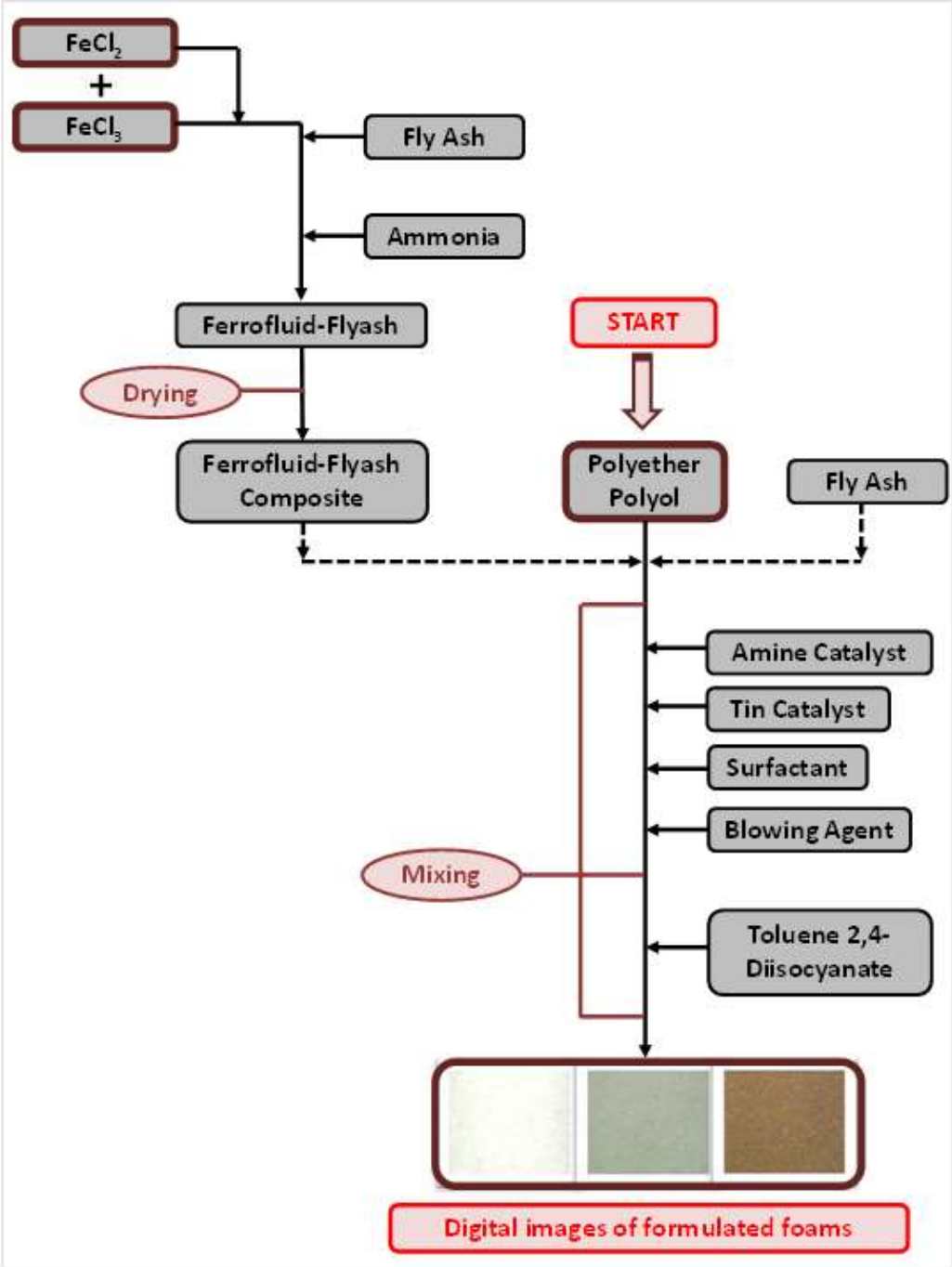

Fig. 19A: Flow Chart for the preparation of polyurethane foam with ferrofluid

In the preparation of PU foam with fly ash incorporated with ferrofluid, first of all, fly ash (10 gms) and activated charcoal (5 gms) is dispersed in ferrofluid (100 ml) and sample is heated so that a uniform powder is obtained. Then in the reaction vessel, 100 gms of polyether polyol (Voranol V3322) was taken to which ferrofluid incorporated

with fly ash and activated charcoal (20 phr) was added and mixed with mechanical stirrer for one hours at the constant speed of 2000 rpm. After that, calculated amount of amine catalyst (0.08 phr), tin catalyst (0.15 phr) and silicon surfactant (1.2 phr) were added and stirred for another 20 seconds at the same speed to ensure homogeneous blend. In this calculated amount of water (2.3 phr) is added and again stirred for 20 seconds at same speed. In a second vessel, calculated amount of TDI (28.8 phr) was taken in another beaker and then poured into first beaker in one shot while stirring continuously for 10 more seconds and then the whole reaction mixture was poured into an open ended cardboard mould. As prepared foam was kept undisturbed for 24 hours to ensure complete curing and was then cut for sample specimen for required shape and size. It was observed that addition of 20 phr flyash incorporated with ferrofluid and activated charcoal increases the tensile strength from 55.11 to 63.24 kPa whereas hardness was found to increase from 32 to 63 (Asker F Scale) and flammability was found to decrease from 81 to 58.1 (FMVS-302). The foam so formed possess magnetic characteristics as well as electrical characteristics and this foam can be used for static charge dissipation as well as may find applications in removal of toxic elements from waste water. The static decay time observed for this foam was found to be 0.85 sec to 0.90 sec.

The effect of various constituents loaded into polyol base with respect to tensile strength, hardness factor, flammability and static decay time data are listed in Table I. It shows that incorporation of flyash increases the tensile strength and hardness factor and flammability of foam composites shows that flame retardency improves when foam is formed alongwith fly-ash, flyash with ferrofluid and flyash with ferrofluid and activated charcoal. Table 7 shows various parameters when flyash is loaded into poly urethane matrix.

Table 7: Effect of loading of flyash, ferrofluid and activated charcoal in polyol base on Tensile strength, hardness factor, flammability and static decay time

Sample	Polyol Used	Loading (phr)	Tensile Strength (kPa)	Hardness Factor (Asker F Scale)	Flammability (FMVSS-302)	Static decay time (sec)
1	V3322	0	55.11	32	81	120 -134
2		20 phr flyash	55.31	53	63	2.83-3.11
3		40phr flyash	65.11	66	61.2	2.02-1.87
4		60phr flyash	52.17	67	50.8	1.01-1.08
5		20 phr flyash+ferrofluid	59.68	61	60.4	2.65-2.98
6.		20 phr flyash+ ferrofluid+ activated charcoal	63.24	63	58.1	0.85 -0.90

*phr stands for parts per hundred of polyether polyol.

**[TDI=9.67x(parts of water) + (0.155 x(OH value)]

*** All the catalyst compositions are taken with respect to base polyol (This procedure is followed throughout the foam formation process)

The human body itself is electromagnetic (at a very low level—around 10 hertz). It's been shown that each one of our cells has its own electromagnetic field (EMF). Maintaining balance in those cellular EMFs is critical to staying healthy. Decades of studies have demonstrated that artificial frequencies higher than 10 hertz can create stress and serious health problems.

Cellphone tower wavelengths, microwaves have a significantly higher frequency than even radio waves. The higher the frequency, the more powerful the wave—and the more powerful effect on biological organisms. (Recall a mobile tower emit microwaves at 1900 MHz). These higher energy waves can actually destroy chemical and molecular bonds, creating chaos in our basic biochemical structures. The negative health effects of EMFs and microwave radiation are well documented.

Cell Tower Radiation Has Also Been Linked To:

- Headaches
- Memory loss
- Low sperm count
- Cancer, birth defects
- Heart conditions
- Alzheimer's.

Fabrication of Tiles for ESD and EMI

Accordingly, the present report provides a process of designing fly ash tiles by incorporating specific filler materials and expanded graphite which can be used for EMI shielding and antistatic behavior depending upon the loading of conducting matrix which ranges from 1 % to 15 %. The method comprising:

- Blending of flyash with specific filler materials and incorporating expanded graphite and compression moulding the mixture in specific dies followed by heat treatment and the like.
- Mixing the flyash in different ratios of expanded graphite ranging from 1 % to 15 % depending upon the end application
- Testing the mechanical strength of the tile and checking the filler behavior on mechanical and electrical behavior.
- Checking the performance of the compression moulded tile under hostile conditions

- Testing the shielding behavior and antistatic behavior as per standard technique.

The flow chart for the preparation of fly-ash tiles incorporated with EG is shown in Fig. 20.

- 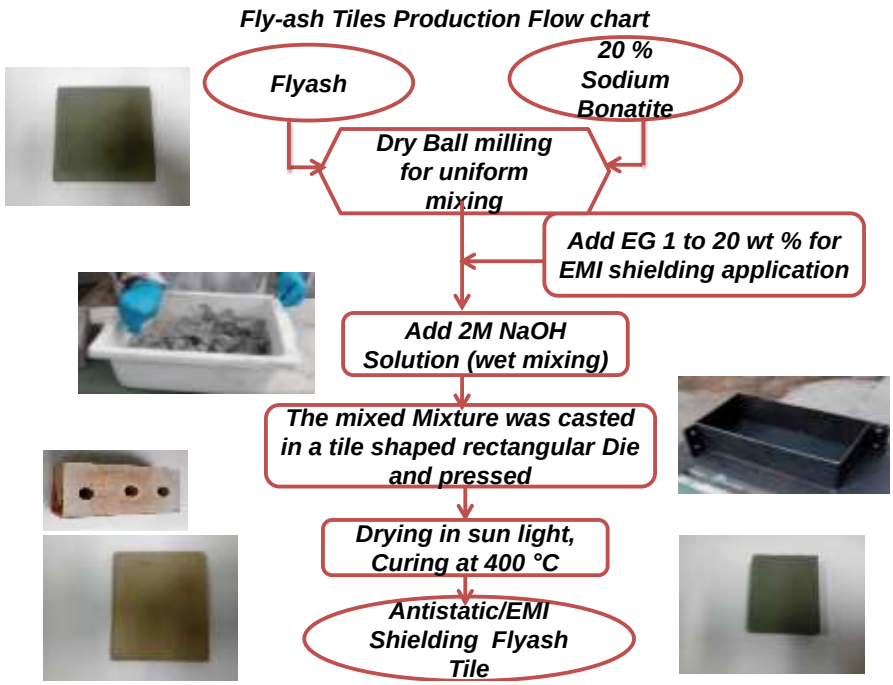

Fig. 20: Flow chart of preparation of Fly-ash tile incorporated with EG

The antistatic behavior of the fly-ash tiles incorporated with 1 % of EG is shown in Fig. 21.

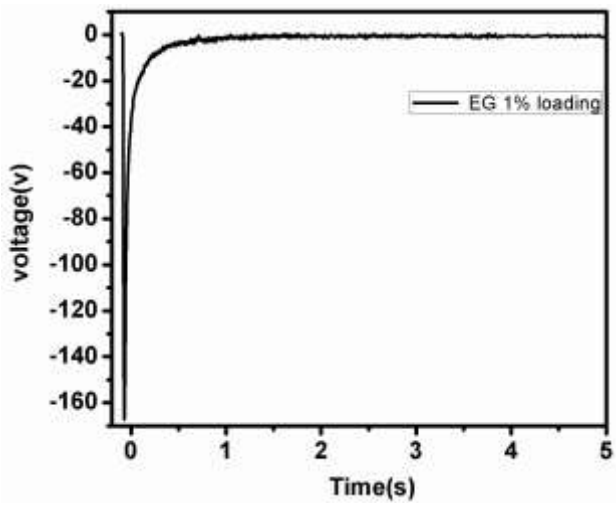

Fig. 21 Antistatic behaviour of Fly-ash composites with 1 % loading

The static decay time data shows that 1 % loading of expanded graphite in fly-ash tile completely dissipates the charge from the surface. Similarly on loading 5% percentage of EG in fly-ash completely dissipates the static charge as shown in Fig. 22. This shows that 1 % loading of EG in fly-ash tile is good enough for using the tile for antistatic purposes.

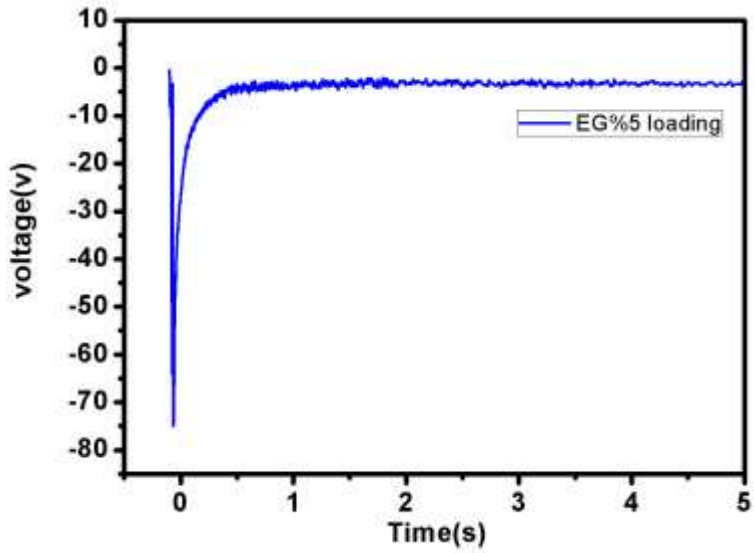

Fig.22: Antistatic behaviour of Fly-ash composites with 5 % loading

EMI shielding behavior of the fly-ash tiles incorporated with different loading levels of EG was also carried out in X-band range in order to see how much shielding attenuation of these tiles can be attained when different loadings of EG is incorporated in the fly-ash tile. Shielding attenuation of these tiles is given in Fig. 23.

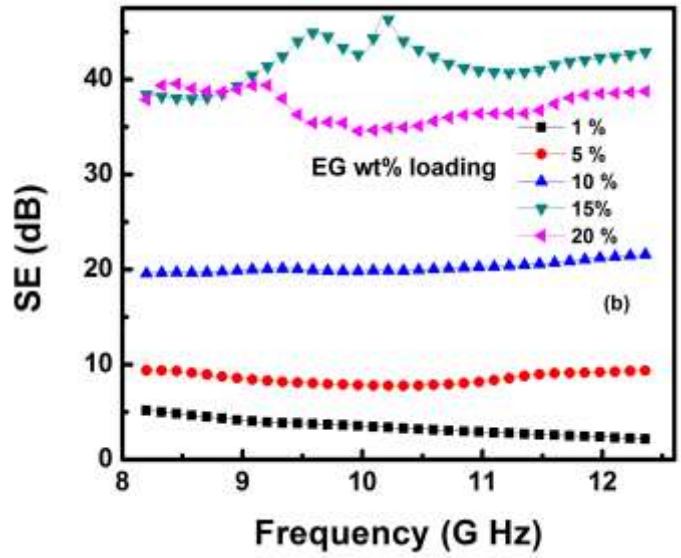

Fig. 23 EMI Shielding behavior of Fly-ash tile incorporated with EG

In-situ synthesis of γ -Fe_2O_3 nanoparticles in fly ash, EG matrix: EGIOFA composite

The synthesis of EGIOFA composite was carried out by the in situ generation of γ-Fe_2O_3 nanoparticles in an EG matrix containing fly-ash particles by chemical reflux method. Prior to EGIOFA synthesis, in a typical process, to obtain graphite intercalated compound (GIC), the natural graphite powder (5 g) was dispersed in a 4:1mixture of concentrated H_2SO_4/HNO_3 (160:40 mL) at room temperature and the mixture was put in an ace bath for 1 hour. The addition of a large amount of deionized water (2000 ml) to the above mixture caused violent effervescence and temperature was increased to 50°C, The mixture was then stirred at 65 °C for 24 hours by to form the GIC. The GIC suspension was centrifuged (10000rpm, 30min) and the supernatant was decanted away. The remaining solid material was then washed two times in succession with 200 mL of water, 200 mL of ethanol. For each wash, the mixture was centrifuged (10000 rpm for 30 min) and the supernatant decanted away. The paste collected was dried at 100±5 °C in a vacuum oven, which is then rapidly exfoliated at temperatures between 800 and 900°C to form EG. But, it is observed that EG is not transformed in single or double layer graphene sheet because of insufficient oxidation of natural graphite while doing acid treatment or inadequate pressure that builds-up during thermal and chemical exfoliation. Next, EG, iron acetylacetonate, fly ash and ODA were mixed in ethanol and refluxed for 5 hours at 80°C. The subsequent mixture is further heated to 230°C and checked simultaneously with external magnet until the magnetic property appear in the sample. The composites of EG, γ -Fe_2O_3 and fly ash have been formed by fixing 1 wt% of EG, 1 wt% of iron oxide and by varying fly ash ratio from 1, 2, 3, 4 wt% and are abbreviated as EGIOFA1, EGIOFA2, EGIOFA3, EGIOFA4 respectively.

The surface morphology of EG, fly ash and EGIOFA1 have been examined using scanning electron microscope (SEM, Zeiss EVO MA”10) at an acceleration voltage 10.0 kV. The dc electrical conductivity of EG composites has been measured by a standard four-probe

technique on pressed rectangular pallets of dimension 13.0×7.0×1.00± 0.1 mm3 at room temperature in order to eliminate contact resistance effects, using Keithley programmable current source (model 6221) and nano voltmeter (model 2182A). Electromagnetic shielding studies have been carried out using Agilent E8362B Vector Network Analyzer in the 8.2-12.4 GHz (X-band) microwave range. The composite has compacted in a piston cylinder assembly at 60MPa for 5 min into a 2.0 ± 0.2 mm thick rectangle pellet with a dimension to fit the waveguide dimensions. Electromagnetic shielding, dielectric and permeability measurements were carried out on an
Agilent E8362B Vector Network Analyzer in a microwave range of 8.2–12.4GHz (X-band). The prepared PANI-CF composite sheet were cut of the waveguide dimension and inserted in the grove of dimension 22.8 x 10.03 x 3 mm^3 copper sample holder connected between the waveguide flanges of network analyzer. Since the sealing between the specimens and the test fixture is critical and could have a huge impact on the results, therefore we mounted sample holder between adapter and tighten the assembly with the help of screw driver. The set up for measurement is shown in Figure 24 &25.

Figure 24: Right image showing the vector network analyzer for measuring the Scattering parameters and dielectric attributes of the sample while left image showing the Sample holder
fitted between the flanges of the waveguide

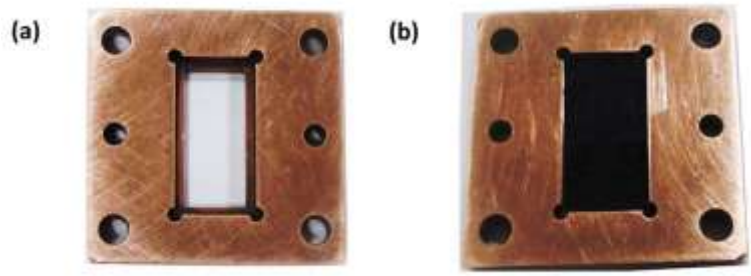

Figure 25. Copper sample holder for measuring the shielding performance (a) without composite sheet (b) a piece of flyash composite sheet fitted in the sample holder.

Schematic representation of incorporation of γ -Fe_2O_3 and fly ash into EG matrix is shown in Scheme 2.

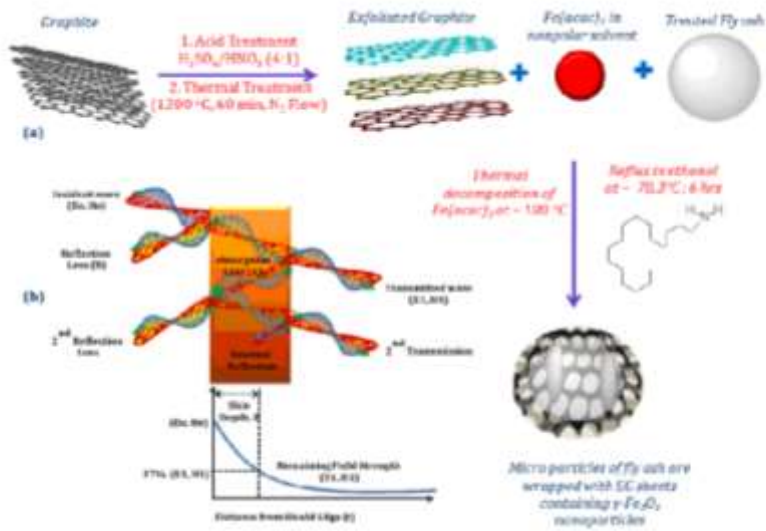

Scheme 2. (a) Schematic representation of preparation of different composites of EG/Ɣ-Fe_2O_3/fly ash by fixing 1 wt% of EG, 1 wt% of iron oxide and with varying ratios of fly ash using ODA as a capping agent in the organic medium (b) illustrates the interaction of electromagnetic wave with the shield.

Fig. 26 shows the dependence of absorption, reflection and total EMI SE with frequency in the 8.2-12.4 GHz range. From the experimental measurement, the shielding effectiveness for the composite EGIOFA due to absorption (SE_A) has been found to vary from 56.45 to 25.01 dB in the composite while the SE_R varies from 3.38 to 7.15 dB for the composites. Thus, the total SE achieved for the fly ash composite is 59.83 dB (EGIOFA1) which is much higher than the pristine fly ash. It has been observed that for conducting EG/ Υ-Fe_2O_3/fly ash composite, shielding effectiveness (SE) is mainly dominated by absorption while the shielding effectiveness due to reflection (SE_R) is constant and contributes comparatively little.

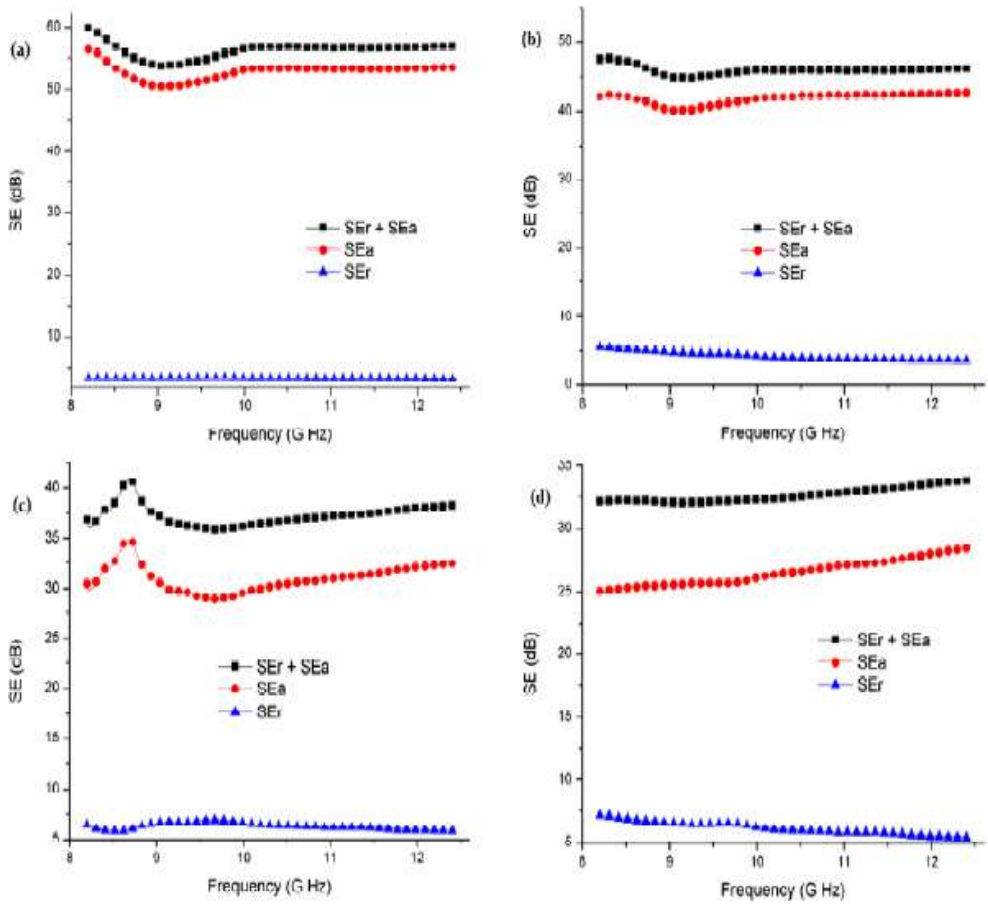

Fig 26. Variation in EMI shielding effectiveness SEA, SER and total SE of (a) EGIOFA1, (b) EGIOFA2, (c) EGIOFA3 and (d) EGIOF4 as a function of frequency

EG and its composite with iron oxide and fly ash (EGIOFA1) have been successfully prepared by using chemical reflux method. The fly ash particles are wrapped with EG layers containing iron oxide nano particles embedded in between the layers enhances the interfacial polarization and the effective anisotropy energy of composite, which contributes to high shielding effectiveness (SE_A~56.4 dB) as compared to conventional fly ash. Addition of nano particles of iron oxide (magnetic filler) and fly ash in the conducting EG matrix gave a new kind of composite materials having better microwave absorption properties (SET~59.83 dB) which strongly depends on weight fraction of iron oxide and fly ash in EG matrix. As a result, fly-ash composite with dielectric core are also promising as new types of microwave absorption materials with usability in radio frequency range maintaining strong absorption. The presence of conducting matrix, magnetic filler and dielectric are helpful for proper impedance matching, which is necessary for enhancing the absorption of the electromagnetic wave. These exceptional properties of new composite using waste fly ash which is byproduct of coal based thermal power stations; assure that it could be an ultimate choice for future building block of EMI SE applications.

REFERENCES

1. Ronnen Levinson, Hashem Akbari and Joseph C. Reilly, Building and Environment, Vol. 42(7), 2007, 2591-2605.
2. Shiao, Ming Liang, Jacobs, Gregory F., Kalkanoglu, Husnu M., U.S. Patent No. 10/749680, 2005.
3. Shiao, Ming Liang, Kalkanogolu, Husnu M., Hong Keith C., U.S. Patent No. 20080008832, 2008.
4. Ja Eun Song, Young Hwan Kim and Young soo kang, Current Applied Physics, 6(2006), 791-795.
5. Ronnen Levinson, Hashem Akbari and Joseph C. Reilly, Building and Environment, Vol. 42(7), 2007, 2591-2605.
6. Paul Berdahl, Energy and Buildings, 22, 1995, 187-191.
7. Hirpmitsu, Y; Yoshiyuki, Z; Hisap O.; Tohru, H.; Yoshio A.; Michiei, N. Eur. Pat. Appl. 1, 217, 044, 2002.
8. H. Yanagimoto et al. US patent 6, 521, 038, 2003.

9. Ashwini K. Bendiganavale and Vinod C. Malshe, Recent Patents on Chemical Engineering, 2008, 1, 67-79.
10. K.J. Sreeram, C.P. Aby, B.U. Nair and T. Ramasami, Solar energy materials and solar cells, 92 (11), 2008, 1462-1467.

11. A.P. Singh, P. Garg, F. Alam, K. Singh, R.B. Mathur, R.P. Tandon, A. Chandra, S.K. Dhawan, "Phenolic resin-based composite sheets filled with mixtures of reduced graphene oxide, ϒ-Fe_2O_3 and carbon fibers for excellent electromagnetic interference shielding in the X-band", Carbon, 50 (2012) 3868–3875.

12. K.-Y. Park, J.-H. Han, S.-B. Lee, J.-B. Kim, J.-W. Yi, S.-K. Lee, "Fabrication and electromagnetic characteristics of microwave absorbers containing carbon nanofibers and NiFe particles", Composites Science and Technology, 69 (2009) 1271-1278.

13. G. Tong, W. Wu, Q. Hua, Y. Miao, J. Guan, H. Qian, "Enhanced electromagnetic characteristics of carbon nanotubes/carbonyl iron powders complex absorbers in 2-18 GHz ranges", Journal of Alloys and Compounds, 509 (2011) 451-456.

14. T. GuoXiu, Y. JinHao, M. Ji, Q.M. Yue, G.J. Guo, L.L. Chao, G. PeiJun, C. JianJing, "Facile preparation and electromagnetic characteristics of Fe/expanded graphite intercalation compounds, SCIENTIA SINICA Chimica, 41 (2011) 1121-1126.

15. N.C. Das, D. Khastgir, T.K. Chakia, A. Chakraborty, "Electromagnetic interference shielding effectiveness of carbon black and carbon fibre filled EVA and NR based composites", Composites Part A: Applied Science and Manufacturing, 31(2000) 1069-1081.

16. D.D.L. Chung, "Electromagnetic interference shielding effectiveness of carbon materials", Carbon, 39 (2001) 279-285.

17. A.P. Singh, M. Mishra, A. Chandra, S.K. Dhawan,"Graphene oxide/ferrofluid/cement composites for electromagnetic interference shielding application", Nanotechnology, 22 (2011) 9

18. S. Yang, K. Lozano, A. Lomeli, H.D. Foltz, R. Jones, "Electromagnetic interference shielding effectiveness of carbon nanofiber/LCP composites Composites", Part A: Applied Science and Manufacturing, 36 (2005) 691 -697.

19. L. Li, D.D.L. Chung, "Electrical and mechanical properties of electrically conductive polyethersulfone composites", Composites, 25 (1994) 215-224.

20. J. Joo, A.J. Epstein, Electromagnetic radiation shielding by intrinsically conducting polymers, Applied Physics Letters, 65 (1994) 2278.

21. C.Y. Lee, H.G. Song, K.S. Jang, E.J. Oh, A.J. Epstein, J. Joo, "Electromagnetic interference shielding efficiency of polyaniline mixtures and multilayer films", Synthetic Metals, 102 (1999) 1346-1349.

22. Y. Huang, N. Li, Y. Ma, F. Du, F. Li, X. He, X. Lin, H. Gao, Y. Chen, The influence of single-walled carbon nanotube structure on the electromagnetic interference shielding efficiency of its epoxy composites, Carbon, 45 (2007) 1614-1621.

23. N. Li, Y. Huang, F. Du, X. He, X. Lin, H. Gao, Y. Ma, F. Li, Y. Chen, P.C. Eklund, Electromagnetic Interference (EMI) Shielding of Single-Walled Carbon Nanotube Epoxy Composites, Nano Lett, 6 (2006) 1141-1145.

24. G. Eda, M. Chhowalla, "Graphene-based Composite Thin Films for Electronics", NanoLett, 9 (2) (2009) 814-818.

25. X. Fu, D.D.L. Chung, "Submicron carbon filament cement-matrix composites for electromagnetic interference shielding" , Cement and Concrete Research, 26 (1996) 1467-1472.

26. Y.H. Jianfeng Shen, Min Shi, Na Li, Hongwei Ma and Mingxin Ye, "One Step Synthesis of Graphene Oxide" Magnetic Nanoparticle Composite, J. Phys. Chem. C, 114 (3) (2010) 1498-1503.

27. H. He, C. Gao, "Supraparamagnetic, Conductive, and Processable Multifunctional Graphene Nanosheets Coated with High-Density Fe_3O_4 Nanoparticles", Appl.Mater. Interfaces, 2 (11) (2010) 3201-3210.

28. V. Chandra, J. Park, Y. Chun, J.W. Lee, I.-C.Hwang, K.S. Kim, Water-Dispersible Magnetite-Reduced Graphene Oxide Composites for Arsenic Removal, ACS Nano, 4 (2010) 3979-3986.

29. J. Liang, Y. Xu, D. Sui, L. Zhang, Y. Huang, Y. Ma, F. Li, Y. Chen, "Flexible, Magnetic, and Electrically Conductive Graphene/ Fe_3O_4 Paper and Its Application for Magnetic- Controlled Switches", J. Phys. Chem. C, 114 (2010) 17465-17471.

30. M. Mishra, A.P. Singh, S.K. Dhawan, Expanded graphite-nanoferrite-fly ash composites for shielding of electromagnetic pollution, Journal of Alloys and Compounds, 557 (2013) 244-251.

31. A.P. Singh, A.K. S., Amita Chandra, S. K.Dhawan, “Conduction mechanism in Polyaniline-flyash composite material for shielding against electromagnetic radiation in X-band & Ku band”, AIP Advances, 1 (2011) 022147.

32. S.R. Dhakate, S.S.M. Borah, R.B. Mathur, T.L.Dhami, “Expanded graphite based electrically conductive composites as bipolar plate for PEM fuel cell”, Inter J Hydro Energy, 33 (2008) 7146-7152.

33. S.R. Dhakate, N. Chauhan, S. Sharma, J.Tawale, S.S. b, P.D. Sahare, R.B. Mathur, “An approach to produce single and double layer graphene from re-exfoliation of expanded graphite”, Carbon, 49 (2011) 1946-1054.

34. G. Tong, Q. Hu, W. Wu, W. Li, H. Qian, Y. Liang, “Submicrometer-sized NiO octahedra:facile one-pot solid synthesis, formation mechanism, and chemical conversion into Ni octahedra with excellent microwave-absorbing properties”, Journal of Materials Chemistry, 22 (2012) 17494.

35. G. Tong, J. Yuan, W. Wu, Q. Hu, H. Qian, L. Li, J. Shen, “Flower-like Co superstructures: Morphology and phase evolution mechanism and novel microwave electromagnetic characteristics”, Cryst. Eng. Comm, 14 (2012).

36. G.-X. Tong, J.-H. Yuan, J. Ma, J.-G. Guan, W.-H. Wu, L.-C. Li, R. Qiao, “Polymorphous Fe/FexOy composites: One-step oxidation preparation, composition control, and static magnetic and electromagnetic characteristics”, Materials Chemistry and Physics 129 (2011) 1189-1194.

37. H. Fang, Y. Wu, J. Zhao, J. Zhu, “Silver catalysis in the fabrication of silicon nanowire arrays “, Nanotechnology, 17 (2006) 3768.

38. N.F. Colaneri, L.W. Shacklette, “EMI Shielding Measurements of Conductive Polymer Blends”, IEEE Trans. Instrum. H.W. Ott, in: Electromagnetic Compatibility Meas., 41 (1992) 29. Engineering, Wiley, New Jersey, 2009.

Major Outcomes of the Project:

1. **Title of the Project**: Modification & Designing of Fly-ash composites in Building Materials for Energy Conservation & Shielding Applications
2. **Participating Labs/Institutes**:(i) CSIR – National Physical Laboratory, New Delhi
   (ii) Amity University, Noida
3. **Objective:**

The main objective of the proposal is to develop infrared reflective coatings by utilizing waste material (fly ash) as substrate coated with an IR reflective material and development of fly-ash composites for EMI shielding applications. The work component includes:

a) Grading and purification of fly ash.
b) Coating of fly ash particles with suitable NIR reflecting material
c) Development and use of paint/ coating formulation
d) Characterization of coatings for their NIR reflective characteristics
e) Synthesis of fly-ash composites by incorporating other filler materials and their characterization for their application in shielding of electromagnetic waves in X-band.
f) Study of shielding effectiveness of composites in microwave range

Achievements:

(i) Electromagnetic foam incorporated with fly ash, ferrofluid and activated charcoal
Waste fly ash has been utilized as filler in poly urethane foam matrix alongwith ferrofluid and activated charcoal so that the resultant flexible foam can be used for ESD and magnetic foam.

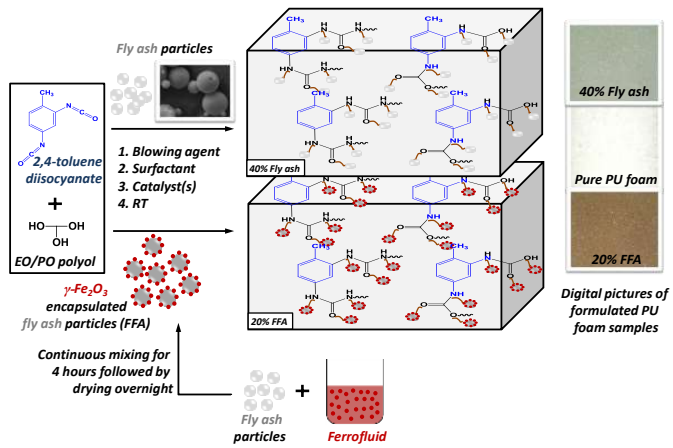

(ii) Flyash as filler in multiphase composite with MWCNT and ferrofluid for shielding of electromagnetic radiation in X-band and Ku-band

Multiphase composites consisting of flyash, ferrofluid and MWCNTs have been prepared for efficient microwave shielding with different composition by utilizing the fly ash a waste material from various industries. This composition has been optimized and found MPC1 (1:2:1) better microwave shielding material where 48 dB of EMI shielding achieved in 12.4-18 GHz frequency (Ku band).

(iii) Control of oil spill in Marine Environment using modified composites

The present invention relates to the preparation of modified composites by incorporating fly ash, activated charcoal and red mud in the matrix which is embedded with ferrite materials in the presence of suitable surfactants which can be used for removal of crude oil spill in marine environment.

(iv) Utilization of flyash as an IR reflective material in paints and development of NIR reflective coatings

The surface modification of flyash is done by coating it with metal oxide i.e. TiO_2 through a simple and economic process and then coatings were prepared by coating this material on the mild steel panels by spray coating technique. This work has led to development of energy efficient coatings based on industrial waste with an added advantage of being antiabrasive and anticorrosive in nature

(v) Solar Reflective Index of Powder samples:

TiO_2 coated flyash prepared by aqueous method I exhibits highest SRI value of 92 as compared other materials indicating it to be good NIR reflective materials. TiO_2 coated Fly ash composite particles prepared using In-situ Precipitation - solvent based method and Aqueous method shows promising results making them potential candidate for using it in a cool pigment. But the core-shell composites prepared by using Aqueous method has advantages over In-situ Precipitation - solvent based method as it is solvent free method hence environmental friendly. The difficulty in dispersion of Fly ash during coating process was solved in aqueous method where it was dispersed through ultra-sonication and therefore more uniform coating of TiO_2 on Fly ash was obtained.

Patents Filed: Three + Two
Papers Published: 6 +2

Project Team

From National Physical Laboratory, New Delhi

1. Dr. S.K. Dhawan
   Chief Scientist
   CSIR-National Physical Laboratory
   New Delhi-110012
   skdhawan@mail.nplindia.org

2. Mr. Brijesh Sharma
   Technical Officer
   CSIR-National Physical Laboratory
   New Delhi-110012
   brijeshsharma31@gmail.com

3. Mr. Pradeep Sambyal
   Project Assistant
   CSIR-National Physical Laboratory
   New Delhi-110012
   pradeepsambyal23@gmail.com

From Amity University, Noida

1. Dr. Sangeeta Tiwari
   Amity Institute of Applied Sciences (AIAS)
   Room No.429, E1 Block, IVth Floor
   Amity University Uttar Pradesh
   Noida-201 303
   stiwari2@amity.edu

2. Ms. Richa Sharma
   Project Fellow
   Amity Institute of Applied Sciences (AIAS)
   Amity University Uttar Pradesh
   Noida-201 303
   richasharma.rs89@gmail.com

Project Monitoring Committee

1. **Prof. D. Kumar**
   Chairman, Project Monitoring Committee
   Head, Department of Applied Chemistry & Polymer Technology
   Delhi Technological University
   Bawana Road, Delhi-42
   dkumar@dce.ac.in

2. **Prof. Veena Choudhary**
   Centre for Polymer Science & Engineering
   Indian Institute of Technology
   Hauz Khas, New Delhi-110016
   veenach@hotmail.com

3. **Dr. M.K. Kamat**
   CEO
   M/s Krishna Conchem Products Pvt. Ltd.
   #2, Bldg #6, Sector 3, Millennium Business Park,
   Mahape, Navi Mumbai- 400710
   madankamat@gmail.com

4. **Dr. Sanjeev Palliwal**
   Central Pollution Control Board
   New Delhi

5. **Dr. Fehmeeda Khatoon**
   Department of Applied Sciences
   Jamia Millia Islamia University
   Delhi-110025
   fehmeeda58@gmail.com

6. **Dr. M. Raina**
   Director/Scientist F - Member Secretary, MoEF
   Ministry of Environment & Forest and Climate Change
   Room No. 215, Prithvi Block,
   Indira Paryavaran Bhawan
   Jor Bagh, New Delhi-110003
   mraina@nic.in